GEOMETRICALLY PROJECTED DISCRETE DISLOCATION DYNAMICS

By

Shamseddin Akhondzadeh

A dissertation submitted to the Johns Hopkins University in conformity with the requirements for the degree of Master of Science in Engineering

Baltimore, Maryland

August, 2016

Geometrically Projected
Discrete Dislocation Dynamics

by

Shamseddin Akhondzadeh

Submitted to the Department of Civil Engineering at Johns Hopkins University in conformity with the requirements for the degree of Mater of Science in Engineering

Abstract

Plastic deformation of crystalline materials is due to the motion of large numbers of dislocations, which are line defects in the crystal's atomic structure. Various macroscopic properties of deformed crystalline solids may be predicted by studying the motion of dislocations, namely yielding, ductility, creep as well as fatigue.

Dislocations are defined at the atomic scale, but modeling all atoms using an atomistic simulation approach is prohibitively expensive. Instead, by considering dislocations as carriers of plastic deformation in a crystal, one may minimally simulate the dynamics of dislocation lines in a continuous elastic medium.

Three dimensional discrete dislocation dynamics methods (3D-DDD) have been developed to explicitly track the motion of dislocation lines under applied stress. However, the principal limitations of these methods are the insurmountable computational cost required to complete a full scale simulation and process its results, due to various issues such as dislocation multiplication, dislocation reactions and interactions with obstacles. It is common that 3D-DDD simulations are

mostly limited to trivial structural and pattern information, sub-micron length scales and short durations, usually requiring hundreds of processors and TB storage units. Spatial and temporal 3D-DDD post simulation analysis is typically a multi-year project. These limitations enforce the construction of multiscale minimal approaches to efficiently simulate the motion of dislocations for large length and time scales, in ways that patterning and correlation effects can be pursued.

In the present thesis, a minimal multiscale approach is presented with considerably less computational cost to simulate dislocations' motion in crystals. We propose the Geometrically Projected Discrete Dislocation Dynamics (GPDDD), where dislocation loops are modeled at every time step, through a set of shapes that form a geometric symmetry group, given the possible mutual operations that dislocation dynamics allows. The simplest version of GPDDD considers only rectangle loops, composed of two screws and two edge dislocation segments in their respective slip plane. We present the case of single-slip loading of copper, where we include dislocation sources and obstacles, as well as basic observables that can be directly compared to detailed 3D-DDD simulations using ParaDis. A simulation using GPDDD requires ~1000 times smaller computational processing and storage for a realistic copper single slip-loading loading case, and the requirements do not scale with the number of discretization segments. The method can be readily extended to include cross-slip and other dislocation dynamics mechanisms, similarly to how 3D-DDD methods are typically developed.

Advisers

Profesor Stefanos Papanikolaou

Professor Lori Graham-Brady

Acknowledgments

I would like to take this opportunity to express my gratitude to my advisers Prof. Stefanos Papanikoalou and Prof. Lori Graham-Brady for their continuous support and help during my studies.

I was very fortunate to join Prof. Papanikolaou's group whose guidance, advice and friendship made my task much easier and my time working on my thesis enjoyable and very memorable. I am very grateful to him for including me on this interesting topic, providing me with invaluable guidance through several individual meetings, and helping me walk through every single step of the work.

I am thankful to Prof. Graham-Brady for allowing me to work on this topic and providing me with ever present advice and support.

My appreciation also goes to Dr. Ryan Sills for his time answering all my questions and his great help when I was learning to work with DDLab code.

Last but not least, I would like to thank my family, my parents and my sister, whose love and support even from long distances has always been an encouragement and a motivation to continue in my academic path.

Contents

List of figures

List of tables

Chapter 1

Introduction

1.1 Introduction to crystalline materials

Materials with repeated arrangements of atoms are called crystalline materials, which include metals and many other non-metallic solids. Unlike the crystal structure of alloys and non-metallic solids, crystalline structure of most pure metals are relatively simple. The most common crystal structure of metals are face-centered cubic (FCC), body-centered cubic and close-packed hexagonal (CPH), which are schematically shown in the figure below, by assuming each atom as solid spheres.

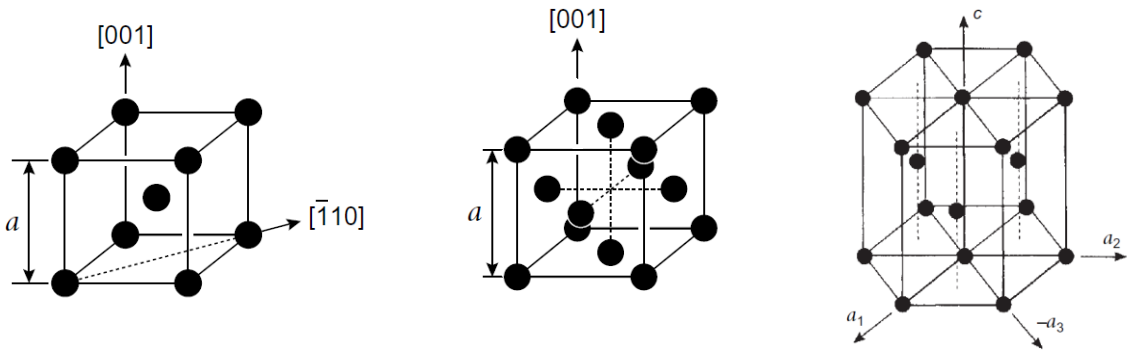

(a) (b) (c)

FIGURE 1-1 CRYSTALLINE STRUCTURE OF ATOMS (A) BCC (B) FCC (C) CPH. [*HULL AND BACON (2011)****]***

Each of the parallelepipeds shown in the above figure is called a unit cell and the metal is made of repetitive arrangements of these cell in three dimensional. Dimension of the unit cells are denoted by lattice parameters and its directions by crystallographic directions. Every direction and plane are described by reference to the crystallographic directions, such that directions are implied by brackets [] and planes are shown by (). If the crystallographic directions of the solid is unchanged to the edges of the sample, solid is called single crystal. On the other hand, polycrystal solids are made of regions where orientation of the cells are different from one another. Each region is called a grain and orientation of crystals in each grain is usually an influential parameter in determining the mechanical properties of solids. In the case of single crystals, mechanical properties of the solid is dependent on the loading direction and thus it is not isotropic. However, response of polycrystals with randomly oriented grains is isotropic and the mechanical properties are provided as single scalars independent on the loading direction. If the orientation of the grains in polycrystals have a favored direction such as cold formed steel, the polycrystal is called textured.

1.2 Dislocations

The arrangement of atoms in a crystalline solid is not always well organized and imperfections may be present. These imperfections might be in the form of point defects such as an extra atom, stacking faults, twin boundaries or dislocations. In this work we are concerned with dislocations, and they can be described as line defects in the crystal structure where atoms are out of position. Dislocation are present even in well-annealed crystals. The presence of dislocations in the atomic structure of metals was inferred from the discrepancy of the shear stress required to plastically deform a single crystal resulted from experimental and theoretical values in the early 1950s. Each dislocation is characterized by its burgers vector, which is defined to represent the lattice distortion, and line direction vector. Burgers vector is denoted by b and line direction by ξ. Based on the direction of b and ξ, relative to each other, dislocations are categorized as edge dislocation, screw dislocation or mixed dislocation.

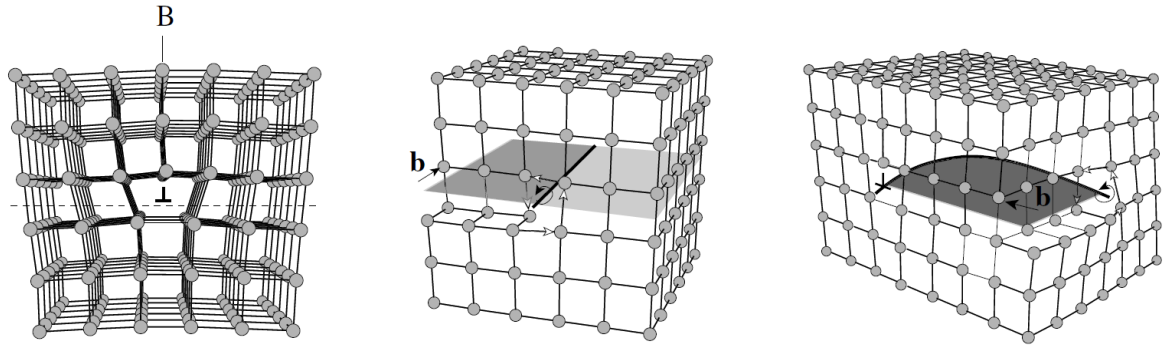

(a) (b) (c)

FIGURE 1-2: DISLOCATIONS IN THE CRYSTAL STRUCTURE OF SOLIDS. (A)EDGE DISLOCATION WITH BURGERS VECTOR AND LINE DIRECTION PERPENDICULAR TO EACH OTHER. (B) SCREW DISLOCATION WITH BURGERS VECTOR AND LINE DIRECTION PARALLEL TO EACH OTHER. (C) CURVED LINE DISLOCATION WITH AN EDGE DISLOCATION AT ONE END , SCREW DISLOCATION AT THE OTHER END AND MIXED DISLOCATION CONFIGURATION IN BETWEEN [BULATOV AND CAI (2006)].

Dislocations can move, multiply and react with each other and in this way, plastic deformation is created in the solid. Dislocations move along certain planes, referred to as slip plane. For an edge dislocation shown in Figure 1-2 with burgers vector perpendicular to its line direction, slip plane is uniquely defined as a plane which contains both of the two vectors and its normal to the plane is $n = b \times \xi$. A slip system is defined by slip direction and slip plane. Usually slip occurs in the close packed planes with high atomic density that is the atoms are very close to each other. This is because atoms moving into another atoms' place in this plane, have the minimum amount of displacements, thus, the energy required to move them is minimum. Close packed planes in a FCC metal are $(111),(\bar{1}11),(1\bar{1}1),(11\bar{1})$ which are collectively shown by $\{111\}$. Also, for FCC metals, in each slip plane, they are three directions with highest density of atoms, for example for (111) three directions are $[1\bar{1}0],[10\bar{1}],[01\bar{1}]$. Collection of these four close packed planes and three direction, result in 12 slip systems for FCC metals. For BCC metals, there are 48 slip systems in total. As for the movement of screw dislocation, since the burgers vector and line direction is parallel to each other, there is no unique plane containing both of the vectors. This is why, screw dislocations can change their glide plane when meeting an obstacle. Change of slip plane of screw dislocation is called cross slip. For instance, in FCC metals, screw dislocation moving in (111) slip plane can switch to $(\bar{1}11)$ slip plane which contains the direction of burgers vector. Movement of edge

dislocations outside the slip plane is also possible under thermally activated conditions, and it is called climb movement.

Dislocations are not always straight line and they can be curves as shown in the Figure 1-2. Along a dislocation line, burgers vector is constant, but the line direction changes. The segments along a curved dislocation, with burgers vector neither parallel nor perpendicular to the line direction is of mixed type. Dislocation loop is an example of this, which can be defined as a closed curved dislocation line. As can be shown in the figure below, the burgers vector is constant along a dislocation loop and the direction of ξ varies. There are two segments with the two vectors parallel to each other which means screw dislocations. Each screw dislocation has a sign associated with it, and by convention, screw dislocation with its two vector in the same direction is called right handed screw dislocation; left handed screw dislocations are segments with the two vectors with opposite directions. Furthermore, positive edge dislocation and negative edge dislocation can be defined similarly.

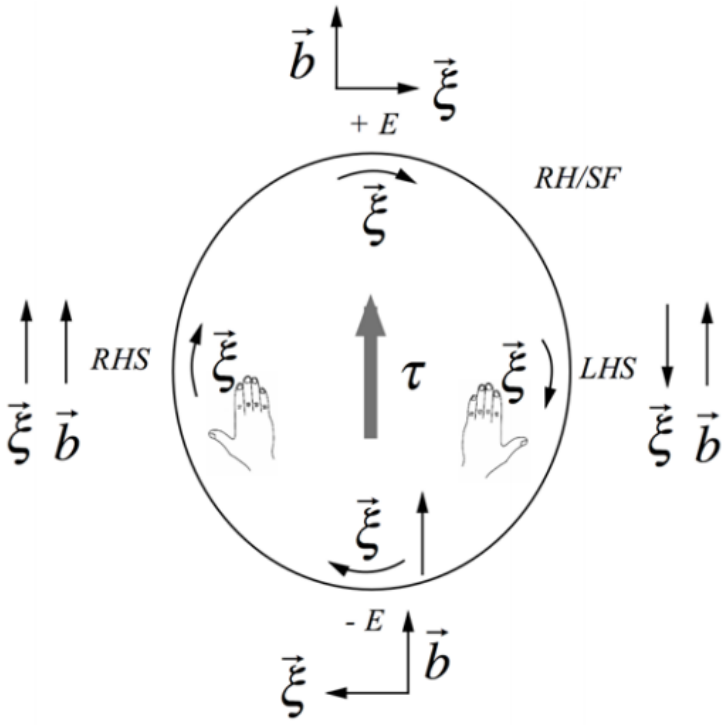

FIGURE 1-3 DISLOCATION LOOP AND THE CONVENTION TO DEFINE SIGN OF A DISLOCATION. [W.D. NIX, PARTIAL DISLOCATIONS TUTORIAL FOR FCC METALS, STANFORD]

Each dislocation has an elastic stress field associated with it. Elastic stress fields for a screw dislocation are [**Hull and bacon (2006)**]:

$$\sigma_{xx} = \sigma_{yy} = \sigma_{zz} = \sigma_{xy} = 0$$
$$\sigma_{xz} = -\frac{Gb}{2\pi}\frac{\sin\theta}{r} \qquad 1\text{-}1$$
$$\sigma_{yz} = \frac{Gb}{2\pi}\frac{\cos\theta}{r}$$

where r,θ are calculated from position of the dislocation in the glide plane based on the direction of the dislocation. Stress fields for edge dislocation are **[Hull and bacon (2006)]**:

$$\sigma_{xz} = \sigma_{yz} = 0$$
$$\sigma_{xx} = -\frac{Gb}{2\pi(1-\nu)}\gamma\frac{3x^2+y^2}{(x^2+y^2)^2}$$
$$\sigma_{yy} = \frac{Gb}{2\pi(1-\nu)}\gamma\frac{x^2-y^2}{(x^2+y^2)^2} \qquad 1\text{-}2$$
$$\sigma_{xy} = -\frac{Gb}{2\pi(1-\nu)}x\frac{x^2-y^2}{(x^2+y^2)^2}$$

Two dislocation with the opposite sign, attract each other while two dislocations with the same sign repel each other. Also, when one dislocations meets another dislocation with the opposite sign, they will annihilate. This is easy to imagine in case of edge dislocation: positive dislocation means there is extra half plane of atoms on top of the plane and negative edge dislocation represents an extra half plane of atoms to the bottom of the glide plane. If these two dislocations slip on the same plane after collision there is not any more extra half plane of atoms, which means dislocations have annihilated. On the other hand, when two dislocations with the same sign, become closer to each other, dislocations pile up until they could overcome the barrier that prevents them from getting away from each other. This is the case, when one of the dislocations is stuck at an obstacle and an external stress pushes another dislocation forward, close to the first dislocation.

Forces on the dislocations can be calculated based on the well-known Peach-Koehler formula:

$$\mathbf{f}(\mathbf{x}) = (\sigma(\mathbf{x}).\mathbf{b}) \times \xi(\mathbf{x}) \qquad 1\text{-}3$$

where $\mathbf{f}(\mathbf{x})$ is the force per unit length on the dislocation and $\sigma(\mathbf{x})$ is the stress filed imposed on the dislocation. This relationship implies that forces on the dislocation is always perpendicular to the line direction of dislocation. Considering a dislocation loop and the Peach-Koehler relation on its segments, it can be deduced that forces on the loop are always in the direction of expanding or shrinking. For example, let's assume a dislocation loop on *xz* plane with its normal vector, $n=[010]$ and burgers vector in the direction of *x*, as $b=[100]$. If shear stress of $\sigma_{xy}=1$ is applied on the loop, based on the PK force relationship, forces on the loop are $\mathbf{f}(\mathbf{x})=[010]\times\xi(\mathbf{x})$ and it is an inplane force perpendicular to $\xi(\mathbf{x})$, which means it is tangent to the loop and will either expand or shrink the loop.

1.3 Dislocation models at different length scales

Dislocations are defined at the atomic scale and depending on the type of problem at hand, they can be modeled at three different length scales: atomistic, continuum and an intermediate length scale referred to as mesoscale. Below is a brief summary of each of these regimes.

1.3.1 Atomistic length scale

At this scale atoms which are building blocks of materials are explicitly simulated in order to derive fundamental properties of solids. Molecular Dynamics (MD) and Monte Carlo (MC) simulations lie in this category. At this level goal is to model the motion of individual atoms through integrating classical Newton's equation of motion. Using this approach, some properties of the material can be determined and used as input in upper length scale simulations. For example, dislocation core behavior or dislocations' drag coefficient in a material which is determined by MD simulations by calculating the velocity of dislocation under applied stress. One of the distinct features of this length scale is being able to model dislocation nucleation. Typical length scale of simulations at this regime using super computers are on the order of hundreds of nanometers containing ~10^{11} atoms. Also time scale range of simulations are less than several nanoseconds.

1.3.2 Continuum length scale

In the continuum model of dislocation, dislocations are not treated as separate objects, but rather as continuously distributed objects in the crystal. Crystal plasticity principles are used to couple

the classical continuum mechanics framework with dislocation distribution to result in continuum dislocation based plasticity. In this approach, position of each dislocation is not considered and thus, dislocation multiplication and annihilation do not happen. Only a small number of dislocation variables such as dislocation density appears in the model. Furthermore, in this regime usually stress-strain response of material is an input to the simulations.

1.3.3 Mesoscale

There may be areas in the solid with high dislocation density, e.g. dislocation pile up or dislocation-free regions, which may play a fundamental role in the failure of the solid. At these points, continuum based models fail to give a good approximation and simulating dislocations as line objects at a smaller length scale is necessary. Various macroscopic properties of deformed crystalline solids may be predicted by studying the dynamics of dislocations, namely yielding, ductility, creep as well as fatigue. Also, simulation of large number of atoms for simulation sizes of more than 1 cubic micron is simply not feasible. Thus, there is a need to simulate dislocation lines and their interaction in meso-scale. Dislocation dynamics (DD) is a modelling approach developed for this purpose and aims to track the motion of dislocation lines under the influence of forces such as applied stress or dislocations' line tension. In discrete dislocation dynamics (DDD) methods, each dislocation line is discretized into straight segments and their motion is tracked through the simulation on much larger scale than MD, typically on the orders of microns and seconds. In this manner, one has access to the position of each dislocation at each instant of time. Also, many important features can be captured such as dislocation pile-ups, dislocation-dislocation interaction and junction formation.

While DDD models has helped to understand many phenomena in crystal plasticity, however, the principal limitations of these methods are the insurmountable computational cost required to complete a full scale simulation and process its results, due to various issues such as dislocation multiplication, dislocation reactions and interactions with obstacles. It is common that 3D-DDD simulations are mostly limited to trivial structural and pattern information, sub-micron length scales and short durations, usually requiring hundreds of processors and TB storage units. Spatial and temporal 3D-DDD post simulation analysis is typically a multi-year project. These limitations enforce the construction of multiscale minimal approaches to efficiently simulate the motion of

dislocations for large length and time scales, in ways that patterning and correlation effects can be pursued.

1.4 Bridge between continuum and DD models

High computational cost of DDD methods necessitates development of minimal models being able to firstly, model each dislocation as separate objects to differ from continuum models; secondly, significantly improves computational efficiency at the same time. Among the minimal models available in the literature, 2dimensional-DDD proposed by **van der Giessen and Needleman (1995)** and 2.5dimensional-DDD introduced by **Gomez-Garcia et al. (2006)** are most popular ones. In the former model, dislocations are assumed as long lines perpendicular to the line direction, which can be assumed as point objects on the simulation plane; this approach is useful to simulate thin film models due to long nature of dislocations. In the latter approach, some mechanisms of 3D-DDD have been introduced in the 2D-DDD model to emulate the dislocation motion in 3D. Both of these approaches are 2 dimensional and movement of parallel dislocations perpendicular to reference plane is tracked on that plane.

In the present thesis, a minimal multiscale approach is presented which is three dimensional in general and needs considerably less computational cost to simulate dislocations' motion in crystals. We propose the Geometrically Projected Discrete Dislocation Dynamics (GPDDD), where dislocation loops are modeled at every time step, through a set of shapes that form a geometric symmetry group, given the possible mutual operations that dislocation dynamics allows. The simplest version of GPDDD considers only rectangle loops, composed of two screws and two edge dislocation segments in their respective slip plane. Surely, the dislocation loop's stress fields and its location is not captured correctly in this way, however, computational efficiency gained by this approximation compensate for this loss of accuracy. Moreover, in a real single crystal solid undergoing plastic deformation, many dislocation loops may be formed, and by assuming each one with a rectangle, errors will average out.

This approach acts as a much needed model to bridge between continuum and mesoscale models. Unlike minimal 2D models, where only edge dislocations are considered, GPDDD models both

screw and edge dislocations. Also contrary to continuum models, it simulates dislocations individually so we can capture phenomena such as dislocation pile-up, etc

A simulation using GPDDD requires ~1000 times smaller computational processing and storage for a realistic copper single slip-loading loading case compared to 3D-DDD, and the requirements do not scale with the number of discretization segments. The method can be readily extended to include cross-slip and other dislocation dynamics mechanisms, similarly to how 3D-DDD methods are typically developed. Another advantage of GPDDD is predicting an initial configuration to be used for 3D-DDD.

The remainder of this thesis is organized as follows. Second chapter summarizes basic features of 3D-DDD and explains the simulation steps, followed by full discussion of GPDDD algorithm. Third chapter depicts dislocation multiplication mechanism in GPDDD. Lastly, chapter four presents the case of single-slip loading of copper, where we include dislocation sources and obstacles, as well as basic observables that can be directly compared to detailed 3D-DDD simulations using ParaDis.

Chapter 2

Discrete dislocation dynamics

2.1 Three dimensional discrete dislocation dynamics

In the three dimensional discrete dislocation dynamics (DD) simulations, each dislocation line is discretized into straight segments with two nodes, and movement of these nodes are tracked and their locations are updated at each time step. In this manner, one has access to the position and velocity of the dislocations at each instant of time during simulation. In this section the method is explained by first summarizing the simulations steps followed by additional aspects of the method.

2.1.1 Basic steps of 3D-DDD

The procedure can be roughly broken down into following steps:

1- Start with an initial configuration of dislocation lines, each dislocation line is discretized into segments based on prescribed values of minimum and maximum segment lengths. Next, each segment is treated as a separate dislocation which carries its own burgers vector and line direction. In this manner, curvature of line dislocations are approximated by several straight segments, and obviously more segments results in better approximation of line dislocation but it comes at an exorbitant computational cost.

Initial configuration in 3D-DDD is usually obtained by assuming straight dislocations in certain angles, and then allowing the system to relax.

2- Forces acting on each node is calculated based on external applied stress, dislocation segments' stress field and line tension using Piech-Koehler formula, as expressed in Eq. (**1-1**1-3)

This step is generally considered to be the most time consuming step in DD simulation as number of segment interactions to be considered is N^2, where N is the total number of segments (**Jie Yin et al. (2012)**).

3-calculation of the node velocities using mobility laws, which relates the nodal forces with nodal velocities by drag coefficients as

$$\mathbf{f}_i = \sum_j \mathbf{B}_{ij}.\mathbf{v}_j \qquad 2\text{-}1$$

where *i* is the node index and *j* denotes the set of nodes connected to *i* as well as node *i.* $\mathbf{B}_{ij}$ is called drag coefficient and they are constant values through simulation. This way, velocity of each node is dependent on the forces acting on that node as well as nodes connected to it by segments. It must be noted mobility laws are different for FCC and BCC materials and this step is where simulation depends on the type of metals. Furthermore, after calculation of velocities at each node, corrections must be made for FCC materials to remove climb components of the nodal velocity to make sure segments remain in their glide plane, and following relation is satisfied

$$\mathbf{v}_i.n_{ij} = 0 \qquad 2\text{-}2$$

where n_{ij} is the normal vector of glide plane of segment *i-j.* All the simulations in this thesis corresponds to single slip system case, thus n_{ij} is constant for all the segments and for simplicity is denoted by n.

4- Time integration is performed to calculate values of nodal displacements, r_i, and then update the location of nodes. Various time integration techniques can be used for this purpose, namely, trapezoid method and Euler forward method, which are examples of implicit and explicit methods. A complete review of time integration techniques are presented in **R. B. Sill and W. Cai (2014).** Next, plastic strains are calculated in this step, based on the following relation:

$$d\varepsilon_{ij}^{p} = \frac{b_i n_j + b_j n_i}{2\Omega} d\mathbf{A} \qquad 2\text{-}3$$

where Ω is the volume of the simulation cell and $d\mathbf{A}$ is the area swept by the dislocation as shown in the following figure.

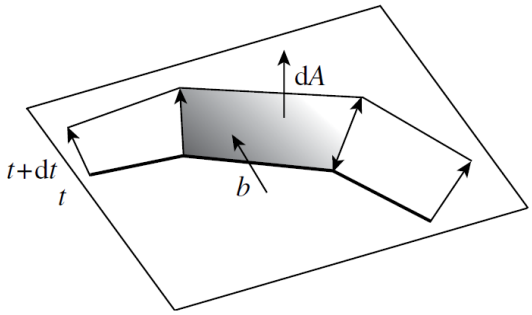

FIGURE 2-1. PLASTIC STRAIN CAUSED BY MOVEMENT OF A DISLOCATION SEGMENT CORRELATES WITH THE AREA IT SWEEPS. [*V. BULATOV AND CAI (2006)****]***

5-New location of nodes are checked for any segment collision and when applicable, segments are split or merged. Also, based on the minimum and maximum values for segment length described in step 1, the segments are remeshed. In this regards, long segments whose length are more than maximum length are cut to two segments, and short segments with length less than minimum are combined with neighboring segments.

6- Finally stresses are updated, based o n the following relations and the procedure is started again for the next time step. Under strain control loading, first a strain rate $\dot{\varepsilon}$ is defined, then, increment of elastic strain is calculated as

$$d\varepsilon^{elastic} = (dt \times \dot{\varepsilon} - d\varepsilon^{plastic}) \qquad 2\text{-}4$$

$d\varepsilon^{plastic}$ is the increment of plastic strain, calculated at step 4 based on Eq. 2-3. Next, applied stress is updated as

$$\sigma_t^{ext} = \sigma_{t+\Delta t}^{ext} + \frac{1}{3}(d\varepsilon^{elastic})_{kk} \times I + 2\mu d\varepsilon^{elastic} \qquad 2\text{-}5$$

2.1.2 Additional features

In the previous fundamentals of DDD simulation were presented. More details regarding the fundamentals of 3D-DDD can be found in **V. Bulatov and Cai (2006)**. Here, we explain two more additional details required for more advanced simulations, dislocation intersection and boundary conditions.

2.1.2.1 Intersection of dislocations

Dislocation networks in a real crystal are distributed among different slip systems. Under applied stress, movement of dislocation on a particular slip system initiates as soon as the amount of shear stress on that system is more than critical value denoted by critical resolved shear stress (CRSS). Thus, dislocations on the slip system with highest shear stress starts moving first. The ratio of resolved shear stress on one slip system to the value of applied stress is known as Schmid factor and the slip system with highest Schmid factor become activated first. As the plastic deformation proceeds, other slip systems are activated too, hence, dislocations from two different slip systems may collide with each other. When a dislocation line intersects with a stationary or mobile dislocation in another plane, two cases might occur. First, dislocations interact with each other and continue their motion, but kinks and jogs are formed on each one of them (**Hull and Bacon (2006)**). Kinks and jogs are defined as steps on the dislocation line which moves the dislocation on the same slip plane and a parallel plane, respectively. Formation of jogs and kinks of two intersecting dislocations depends on the type of dislocation and the direction of burgers vector. For instance, two intersecting edge dislocations on two different slip planes with parallel burgers vector, result in formation of two kinks on each dislocaation equal in direction and length to the burgers vector of the other.

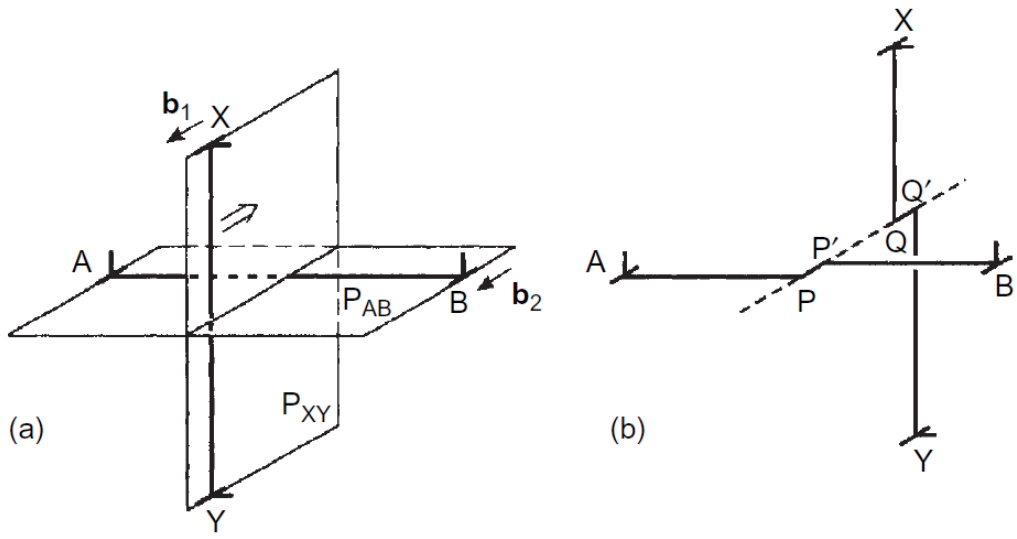

FIGURE 2-2 INTERSECTION OF TWO EDGE DISLOCATION ON DIFFERENT PLANES WITH PARALLEL BURGERS VECTOR. (A) BEFORE COLLISION (B) AFTER COLLISION (HULL AND BACON (2006))

Another case of dislocation intersection is when they zip together and form a junction. After collision of two segments in DDD simulations, determining which of the two cases may occur is based on the energy criterion to ensure that the system obtains maximum dissipation rate.

2.1.2.2 Boundary conditions

An infinite simulation cell size is required to calculate plastic strains based on Eq. (2-3) and similar to any other initial boundary value problem, boundary conditions must be defined for this simulation volume. Periodic boundary conditions can be used by assuming a simulation volume far from any interfaces, such as cracks, grain boundaries, etc, in an infinitely large single crystal. By applying periodic boundary conditions, infinite crystal is replicated by repetitive continuation of simulation volume. This means, for every dislocation in the simulation cell, there are replicas in every other cell known as image dislocations as shown in the following figure. In mathematical form, whenever there is a node at position **r** inside the simulation cell, they are equivalent nodes at positions $\mathbf{r} + n_1\mathbf{L}_x + n_2\mathbf{L}_y + n_3\mathbf{L}_z$ where $(\mathbf{L}_x, \mathbf{L}_y, \mathbf{L}_z)$ are the dimension of the simulation cell and n_1, n_2, n_3 are integers.

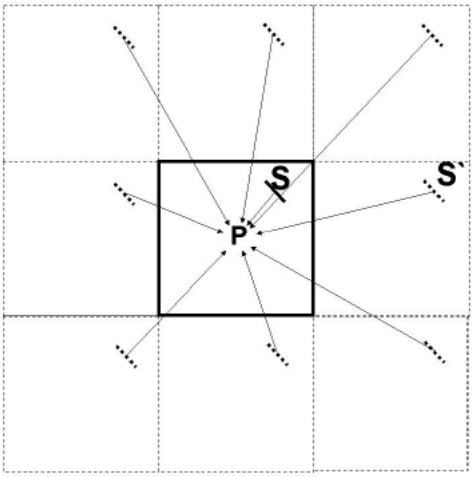

FIGURE 2-3. FOR EVERY DISLOCATION S INSIDE THE SIMULATION CELL, THEY ARE REPLICA DISLOCATIONS AT OTHER CELLS. (V. BULATOV ET AL. (2001))

One important issue to be considered in case of periodic boundary conditions is calculation of stress field due to image stresses. Obviously, direct calculation of forces from image dislocations, even from only neighboring cells is a computationally daunting task. To overcome this difficulty, image forces are approximated based on interpolation between stresses at grid points which are pre-calculated and pre-tabulated (**V. Bulatov et al.(2001)).** More details on the PBC and other types of boundary conditions can be found in **V. Bulatov and W. Cai (2006).**

2.2 Geometrically projected discrete dislocation dynamics

We introduce a novel method for discrete dislocation dynamics which aims to solve fundamental computational and data analysis problems. The major concerns with discrete dislocation dynamics involve the super-exponential explosion of computational cost at large dislocation densities, as well as the explosion of the memory storage requirements. Due to such problems, it has been rather cumbersome to perform clear and reproducible analysis of 3D-DDD. Geometrically Projected Dislocation Dynamics (GPDDD) is a method that optimizes computational cost, which does not depend on the discretization of the dislocation network anymore. GPDDD is based on projections, at every loading time-step, of the dislocation network into a discrete set of shapes that are pre-selected and are consistent with the included dislocation mechanisms. During the progression of the dislocation network, these shapes can expand, combine or transform according to the allowed dislocation mechanisms in the simulation, without generating any new shapes. In this sense, the pre-selected set of shapes should form a discrete mathematical group, where the allowed group operations are all allowed dislocation mechanisms. (**A. Beardon 2012**)

The GPDDD method can be extended in the same way as 3D-DDD, using ab-initio and Molecular Dynamics (MD) results, in order to include further dislocation mechanisms and promote a better description of the atomic-scale deformation of the crystal. The complexity of the GPDDD method primarily amounts to finding a set of geometric shapes that are consistent with the included dislocation mechanisms and evolve self-consistently.

The simplest version of GPDDD consists of approximating dislocation loops with rectangles of screw and edge dislocation to significantly reduce the total number of degrees of freedom. Unlike 3D-DDD simulation, in GPDDD there is no minimum and maximum segment length, remeshing,

splitting, however, other steps of GPDDD simulation is similar to 3D-DDD to a certain extent. The steps are as follows:

2.2.1 Dislocation generation mechanism

As a first step in GPDDD simulation, we need a source to generate loops and for this purpose, we define a dislocation loop source and an activation force corresponding to it. At each time step of simulation, if total forces acting on the source nodes exceeds the source activation force, a rectangle which represents a dislocation loop is added around the source with particular size. Added dislocation loop creates a stress field and impose a force on the dislocation source that prevents it from generating new loops until the first dislocation loop moves away from the source. This procedure is similar to dislocation generation in 2dimensional-DD simulations, where two edge dislocations with opposite signs, are added at opposite sides of a source, when the forces on the source is more than its activation force. By adding a loop around the loop source, we are ignoring all the dislocation motion prior to generation of a loop. For instance, in a frank read source, a segment bows out until a dislocation loop is produced, and there is plastic strain associated with each time step of the segment motion. Thus, in order to account for plastic strain changes when a loop is added, location of the source is considered as the reference location and the plastic strain is calculated based on the location of the new loop with respect to its source. More information on adding a loop around the source and how to define an activation source to emulate Frank-Read source is provided in the next chapter.

2.2.2 Updating the location of nodes

Similar to 3D-DDD, forces acting on the nodes are calculated, then mobility laws are employed to obtain nodal velocities and lastly, nodal displacements are calculated and location of the nodes are updated. It must be noted that location of dislocation source and junctions are fixed throughout the simulation.

Next, each loop is checked to have remained a rectangle or not. If not, it is projected back to a rectangle so that its area is unchanged, using following steps:

- The area and center of the loop is obtained.
- Average length of the opposing side are calculated and used as rectangle lengths

- Rectangle lengths are modified proportional to ratio of two areas to preserve the loop's area

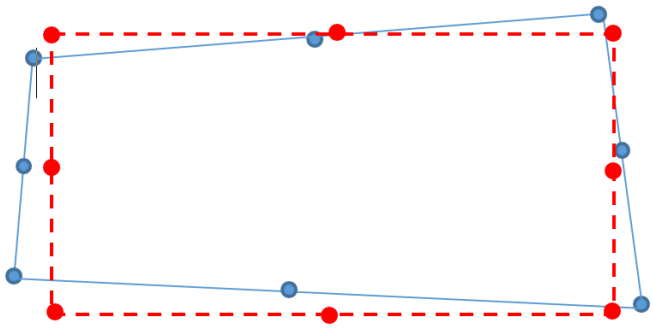

FIGURE 2-4. PROJECTING THE NEW LOCATION OF THE LOOP'S NODES, BACK TO A RECTANGLE.

2.2.3 Collision of segments

Collision function is called to detect any two dislocation segments colliding with each other. Four cases can occur in this step: a) a dislocation segment has collided with an obstacle. b) two separate loops colliding with other. c) one segment of a loop collides with it corresponding segment and causing two line dislocations. d) two line dislocations collide with each other. Each of these case are explained below:

2.2.3.1 Collision of a segment with an obstacle

To hinder the motion of dislocation segments and introduce strain hardening in the stress-strain curves, obstacles are defined. They are defined as separate dislocation with their line vector normal to the glide plane, which is also known as forest dislocation. Similar to loop source, junction nodes' location are fixed and not changed during simulation. In reality kinks and jogs are formed when a segment collides with another off plane segment, but in GPDDD they are not simulated. Off plane dislocations acting as obstacle are handled such that when a segment collides with them for the first time, the segment cannot move closer to obstacle unless the forces acting on its nodes, in the direction of perpendicular to segment line, exceeds obstacle's strength. The procedure is shown in the figure below. Segments that are released from an obstacle, may collide with the same obstacle again, however, after an obstacle release one segment, their subsequent collision will be ignored.

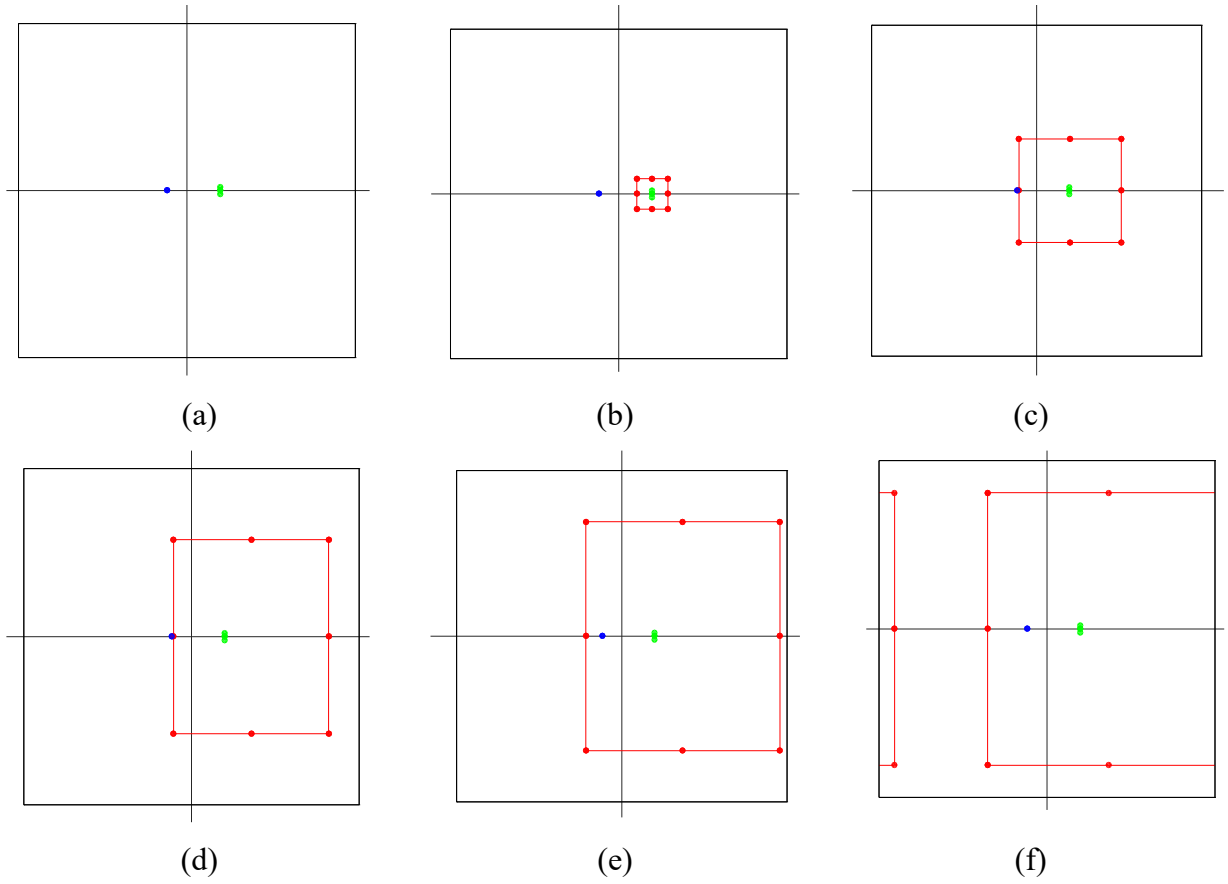

FIGURE 2-5. SIMULATION OF SINGLE SOURCE AND SINGLE OBSTACLE. (A) DISLOCATION LOOP SOURCES ARE SHOWN BY GREEN AND OBSTACLE BY BLUE. (B) ADDING A LOOP AROUND SOURCE WHEN THE SUM OF ITS NODAL FORCES REACHES SOURCE ACTIVATION FORCE. (C) LOOP GROWS UNTIL IT IS STUCK AT A THE OBSTACLE. (D) THE SIDE THAT HAS COLLIDED WITH OBSTACLE DOES NOT MOVE HORIZONTALLY UNTIL ITS HORIZONTAL NODAL FORCES EXCEED OBSTACLE STRENGTH. (E) DISLOCATION SEGMENT HAS BEEN RELEASED FROM THE OBSTACLE. (F) DISLOCATION SEGMENT EXITS THE SIMULATION CELL AND ENTERS THE CELL FROM THE OTHER SIDE SINCE PERIODIC BOUNDARY CONDITIONS ARE APPLIED.

2.2.3.2 Collision of two separate loops

When two separate loops collide with each other, based on the sign of the dislocations colliding with each other two cases might occur. a) dislocation segments have same sign, which can occur when one loop is stuck at an obstacle and an inner loop collides with the loop from inside. It is shown schematically in the Figure 2-6. In this case, merging does not occur, however, a minimum value is imposed for the distance between collided segments. The advantage of having a minimum distance in this case is that as dislocation become very close, their interactions become very strong, and this can lead to very small time steps, thus imposing a minimum distance increases the performance.

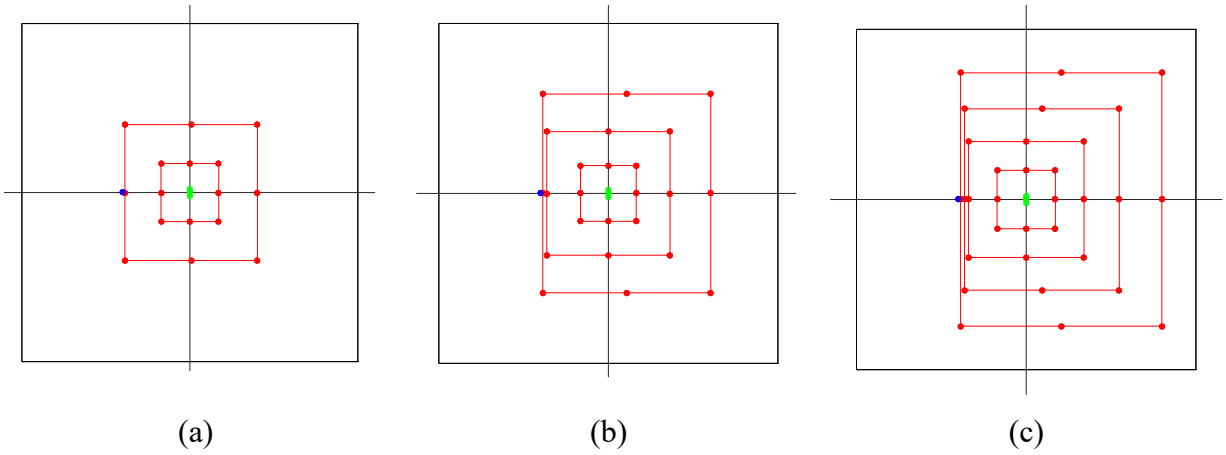

FIGURE 2-6. COLLISION OF TWO LOOPS WITH SEGMENTS OF THE SAME SIGN. (A) FIRST SEGMENT COLLIDES WITH THE OBSTACLE AND ITS HORIZONTAL MOVEMENT IS PREVENTED. (B) SECOND LOOP COLLIDES WITH THE FIRST LOOP, BUT SINCE THE COLLIDED SEGMENTS HAVE SAME SIGN, MERGING DOES NOT OCCUR AND A MINIMUM DISTANCE IS IMPOSED BETWEEN THE SEGMENTS. (C) THIRD LOOP TOUCHES THE SECOND LOOP.

b) dislocation segments with opposite signs collide with each other which results in their annihilation. Thus, when two loops collide with each other and the sign of the collided segments are opposite as shown in the Figure 2-7, collided parts annihilate with each other and one equivalent loop is produced. In GPDDD this equivalent loop will be replaced by a rectangle with the same area to preserve the plastic strain of the system. Replacing two merged loops with one equivalent rectangle follows these steps:

- Area of the two loops are calculated. Also, the furthest two nodes are determined
- Center of the line between two furthest nodes is selected as the center of the new loop and the horizontal and vertical components of the distance between the nodes as the side lengths of the new loop.
- New loop is scaled according to the ratio of the two areas to preserve the area.
- Since this procedure, removes 8 nodes and 8 segments, index of the other nodes and segments must be updated

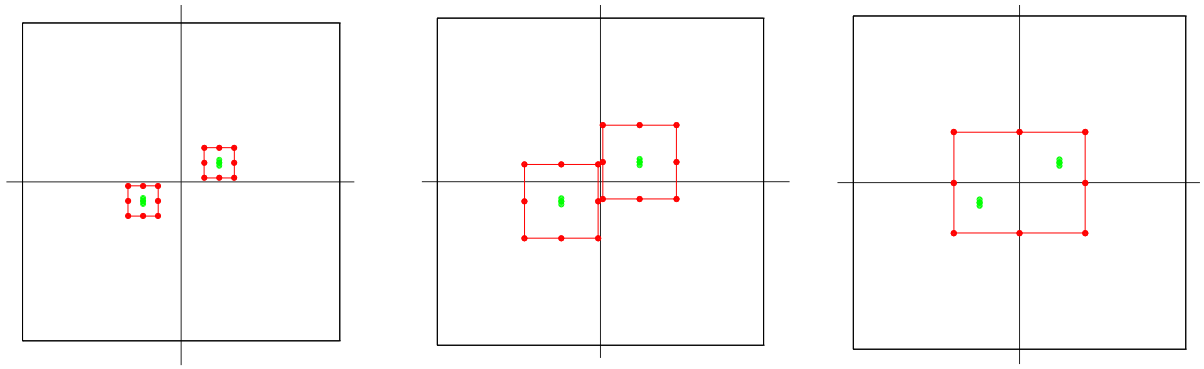

FIGURE 2-7. MERGING OF TWO SEPARATE LOOPS. (A) TWO LOOPS ADDED AROUND TWO SOURCES (B) TWO LOOPS COLLIDE AND THE COLLIDED SEGMENTS HAVE OPPOSITE SIGNS (C) TWO COLLIDED LOOPS MERGE

In some cases, one loop might collide with another loop with some of its segments not in the simulation cell as depicted below. In these cases, the above steps cannot be followed directly, and the loops must be projected back into two rectangles.

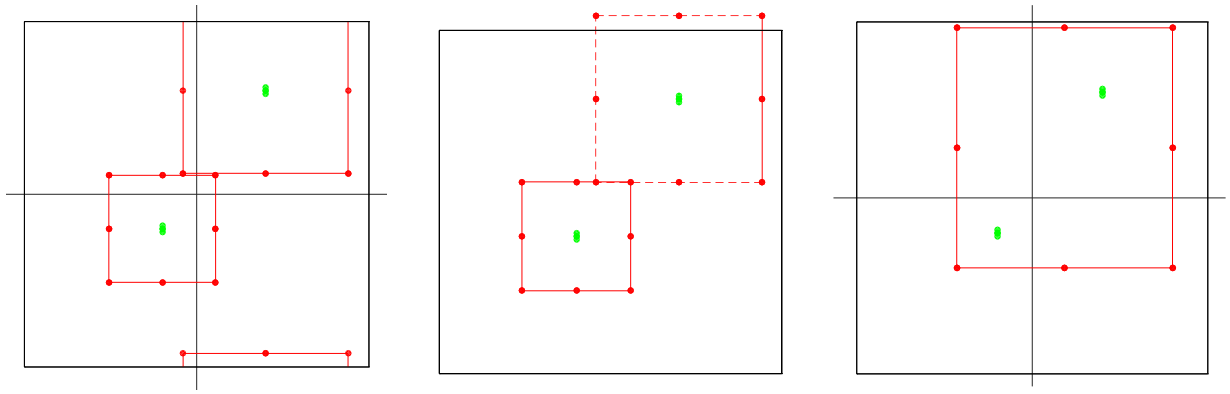

FIGURE 2-8. MERGING OF TWO SEPARATE LOOPS WITH PBC. ALL THREE EVENTS OCCUR IN ONE TIME STEP. (A) TWO LOOPS COLLIDE AND THE COLLIDED SEGMENTS HAVE OPPOSITE SIGNS (B) THE LOOP THAT HAS EXITED THE CELL, HAS BEEN PROJECTED BACK TO A RECTANGLE (C) TWO COLLIDED LOOPS MERGE

Moreover, it is possible that new equivalent loop which replaces the two collided loops, intersects with smaller loops as depicted in the following figure. This will not be permitted by reducing the size of the smaller loops and expanding the bigger loop to keep the aspect ratio of each loop and total area of the loops.

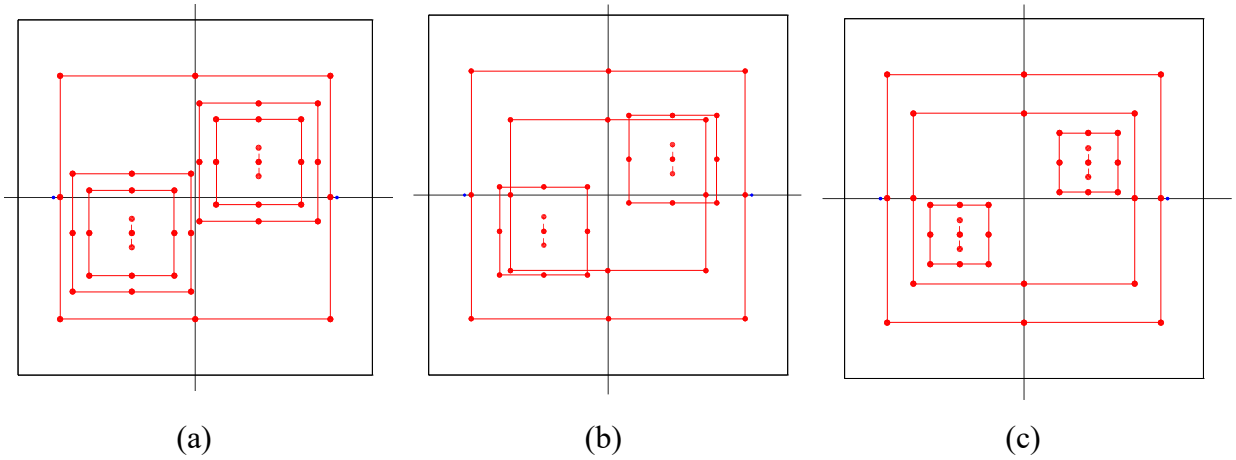

FIGURE 2-9. MERGING OF TWO LOOPS IN THE VICINITY OF OTHER LOOPS. ALL THREE EVENTS OCCUR IN ONE TIME STEP (A) TWO COLLIDED LOOPS. (B) EQUIVALENT NEW LOOP COLLIDES WITH SMALLER LOOPS. (C) SMALLER LOOPS ARE SHRINK AND BIGGER LOOP EXPAND.

2.2.3.3 Loop self-collision

Periodic boundary conditions in DD simulations means dislocations exiting the simulation cell, enter the cell from the other side. So when a segment of a loop exits the cell it enters the cell from the other side, and collides with the segment in the opposing side of the loop. Colliding segments have opposite signs and annihilate since the direction of line vector in the two opposing sides are opposite to each other. Also if there is an obstacle between the two opposing sides, the collision will not happen until one of the segments passes the obstacle. Loop self-collision, results in removing two nodes and four segments, thus, the index of all other nodes and segments must be updated.

2.2.3.4 Two colliding line dislocations

After the loop collides with itself, two opposing sides will annihilate and results in two line dislocations. These two line dislocation may be either screw dislocation or edge dislocation. In case of screw line dislocations, it is assumed that they will still move in the same glide plane and cross slip has not been considered

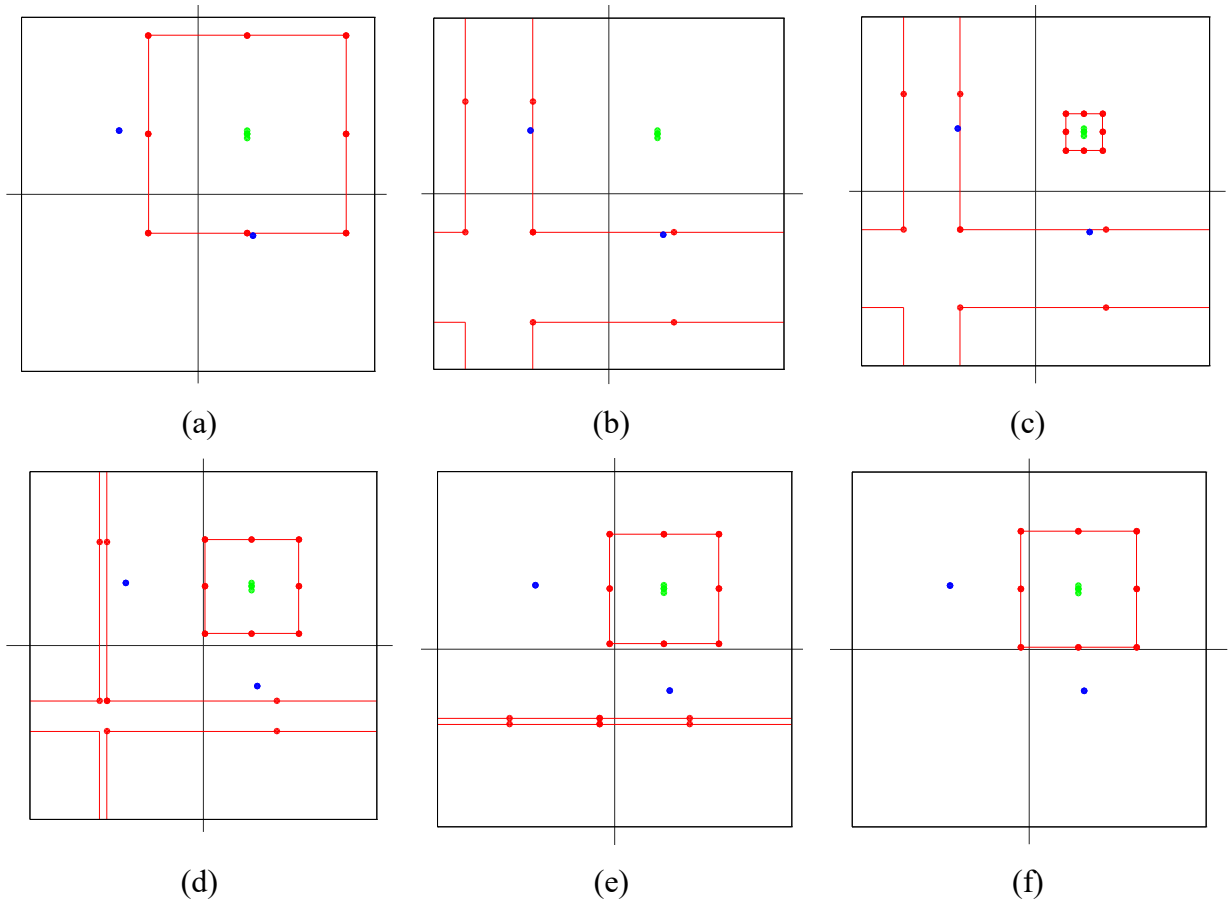

FIGURE 2-10. SIMULATION OF SINGLE SOURCE AND TWO OBSTACLES. (A) FIRST SEGMENT IS STUCK AT ONE OBSTACLE, HENCE IT CANNOT MOVE VERTICALLY BEFORE PASSING THE OBSTACLE (B)SECOND SEGMENT COLLIDES WITH THE SECOND OBSTACLE (C) LOOP SOURCE HAS GENERATED THE SECOND LOOP (D) FIRST LOOP COLLIDES WITH ITSELF, AND VERTICAL SEGMENTS ANNIHILATE. (E) TWO LINE DISLOCATIONS COLLIDE AND SINCE THEIR SIGN ARE OPPOSITE TO EACH OTHER, THEY ANNIHILATE (F) SECOND LOOP CONTINUES TO GROW

2.2.4 Updating stresses

After updating the location of nodes and checking for any collision, merge, obstacles, the plastic strains are calculated based on Eq. 2-3. One issue to consider here, is plastic strain of the annihilated segments, which must be taken into account. For instance, two colliding line dislocations shown in the Figure 2-10(e), cause considerable plastic strain before annihilation and should be accounted for. In the 3D-DDD due to shortness of dislocation segments, the plastic strain before annihilation was ignored. Lastly, stresses are updated similar to the previous case and simulations is continued at the beginning of the next time step.

Chapter 3

Dislocation multiplication mechanism

A deformed crystalline solid can undergo a large amount of plastic deformation under loading. Plastic deformations happen by the movement of dislocations, which means we must have some dislocations in the solid for the plastic deformation to happen. In other words, there must be a mechanism to generate dislocations and to increase the dislocation density in the solid. The best known example of dislocation multiplication is the Frank-Read source, [**Frank and Read 1950**]. When a dislocation is pinned at one end and it is under stress, dislocation acts as a spiral source. Pinning point can be due to any type of barrier, e.g. precipitates, composite jogs or intersection with other dislocations. Dislocations have line tension forces which is similar to surface tension in liquids. For a dislocation pinned at two points, when the forces due to external stress exceeds values from line tension, the dislocation segment starts to bow out. The maximum amount of line tension happens for minimum amount of dislocation curvature that is when the dislocation is semi circle. If the amount of forces acting on the dislocation is more than the maximum line tension, the dislocation is unstable and it further bows out more quickly until two segments of the dislocation line collides with each other. In this case, since the sign of the two collided dislocations are opposite to each other, segments will annihilate and a dislocation loop has been generated from the Frank-Read source. This process is shown schematically in the Figure 3-1.

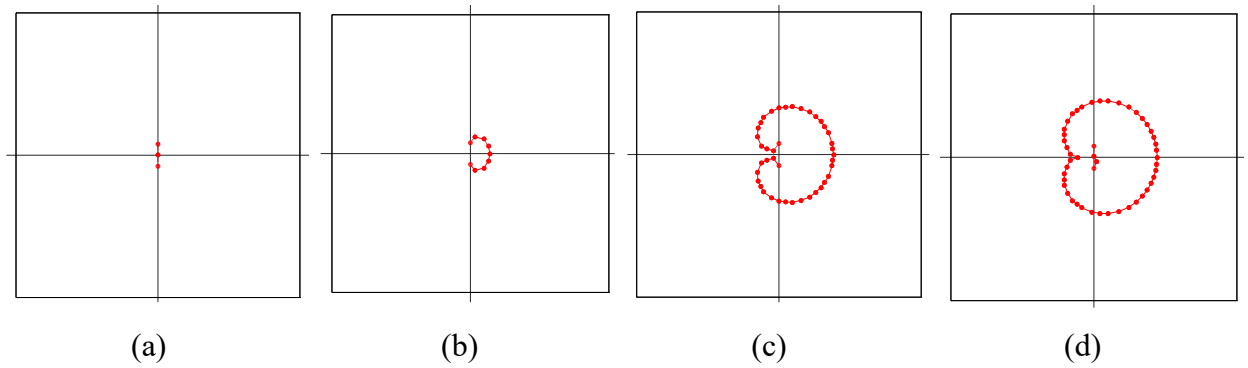

FIGURE 3-1. NUCLEATION OF A DISLOCATION LOOP BY FRANK-READ MECHANISM. (A) A DISLOCATION SEGMENT PINNED AT TWO POINTS. (B) THE DISLOCATION STARTS TO BOW OUT AND THE MAXIMUM RESISTANT BY LINE TENSION IS REACHED WHEN THE DISLOCATION IS SEMICIRCLE. (C) TWO SEGMENTS WITH OPPOSING SIGN COLLIDE. (D) NUCLEATION OF A LOOP AND THE PINNED SEGMENT CONTINUES TO GENERATE MORE LOOPS.

After generation of one loop by Frank-Read segment, the pinned dislocation continues to generate more loops as long as the applied external forces can overcome the line tension. Note that the dislocation loop around the segment, applies forces on the segment, which might prevent further nucleation of loops until the loop moves away from the source. The amount of maximum resistant to bowing out happens at the semi-circle and it depends on the length of the pinned segment. **Estrin et. al. (2007)** showed that this resistance displays a classical Hall-Petch behavior where required shear stress scales linearly with the inverse of the segment length and the trend becomes inverse for larger segments. Presence of Frank-Read mechanism for dislocation multiplication has also been shown experimentally by many researchers, namely by **Kunjomana and Mathai (1991)** as shown in the Figure 3-2.

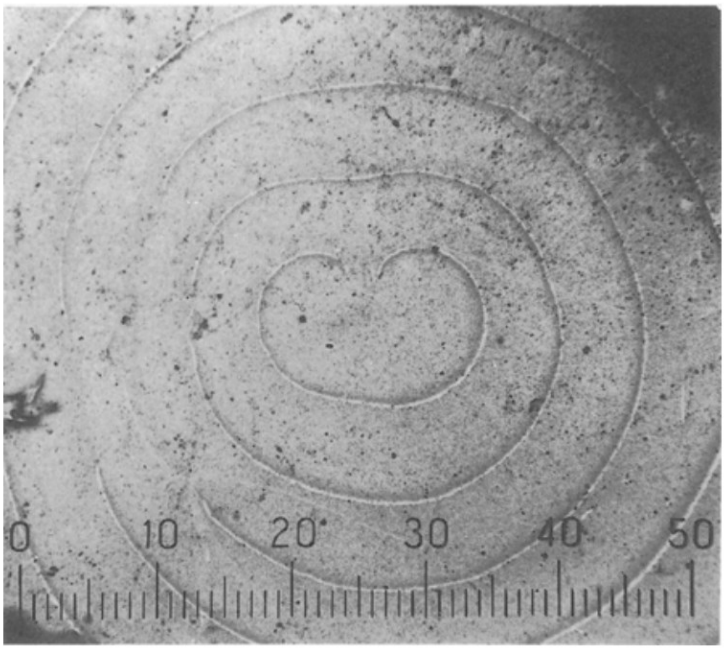

FIGURE 3-2. EXPERIMENTALLY OBSERVED DISLOCATION LOOPS GENERATED FROM FRANK READ SOURCE. [*KUNJOMANA AND MATHAI (1991)****].***

In the present thesis, Frank-Read source mechanism is simulated by assuming a source activation force and time duration required for a source to generate one loop. Bowing out of pinned segment is not simulated as we have only edge and screw dislocations in GPDDD. For this purpose, we define a dislocation loop source as fixed dislocation segment and an activation force corresponding to it. At each time step of simulation, if the total forces acting on the source nodes exceeds the source's activation force, a rectangle which represents a dislocation loop is added around the source with particular size. In this manner, we ignore all the segment's deformation prior to generating a loop. Also there is a time issue to be considered for adding loops –rectangles– around the source. Obviously, Frank-Read source has a time interval associated with generating a new loop. Thus, to simulate the mechanism of Frank-Read source in GPDDD time interval is also considered as well as activation force. To adjust these two parameters in GPDDD according to a Frank-Read source mechanism, 3D-DDD is performed for a segment of 4 μm in a simulation cell of 50 μm. The mechanical properties of copper were used in the simulations as shown in the Table 3-1 [**R. B. Sills et al (2016)**].

TABLE 3-1. MECHANICAL PROPERTIES OF COPPER USED IN THE SIMULATIONS

Property	Parameter	Value
Shear Modulus	μ	54.6 GPa
Poisson's ration	ν	0.324
Burgers vector magnitude	b	0.255 nm
Drag coefficient	B	15.6 $\mu Pa.s$

Periodic boundary conditions were applied to the simulation cell from all sides, and segments exiting the cell during the simulation enter the cell from the opposite side. Segments entering from the other side, collide with their opposite segments of the same loop and since their sign are opposite, they will annihilate. Figure 3-3 shows two steps of the simulations corresponding to strains of 4.1E-4 and 5.6E-4.

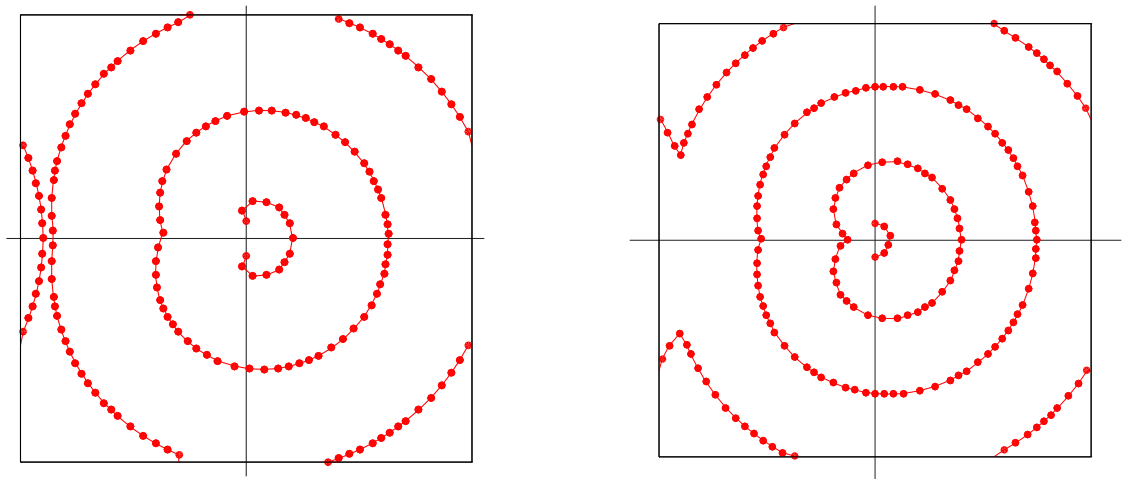

(a) (b)

FIGURE 3-3. 3D-DDD SIMULATION OF A FRANK-READ SOURCE. (A) BIGGER LOOP EXIT THE CELL AND BY PERIODIC BOUNDARY CONDITIONS, ENTERS THE CELL FROM THE OPPOSITE SIDE AND ITS COLLIDING SEGMENTS, ANNIHILATE. STRAIN=4.1E-4. (B) STRAIN=5.6E-4

Single Frank-Read source were simulated subjected to strain rates of 1e3, 2e3, 3e3 and 5e3 in the shear direction, and the Figure 3-4 shows the amounts of total force on the frank-read segment (not considering loops) vs total simulation time.

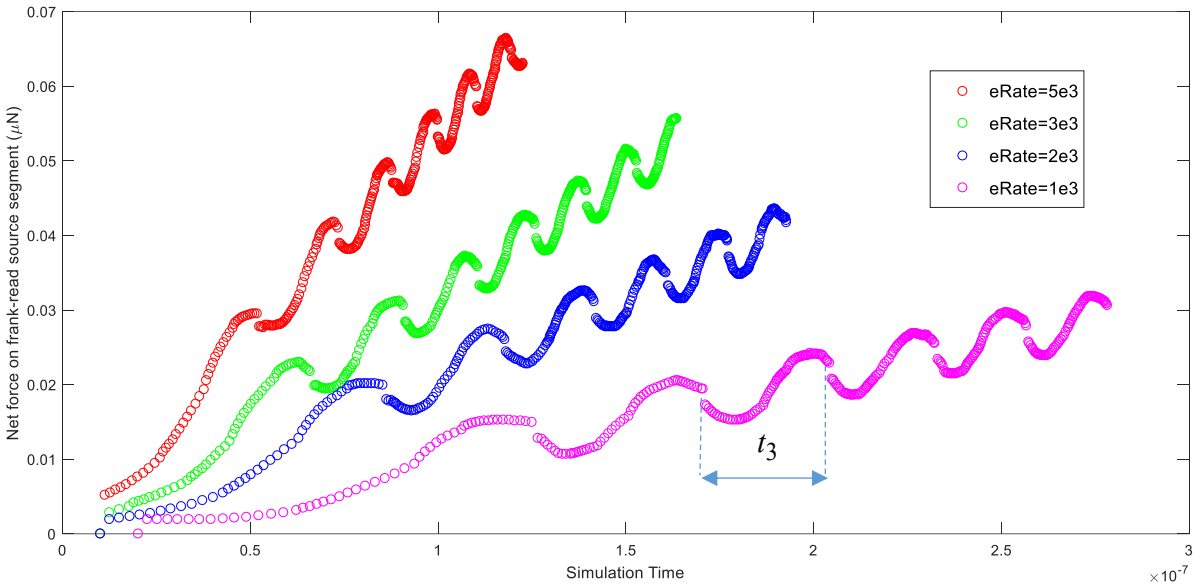

FIGURE 3-4. VARIATION OF TOTAL FORCE ON SINGLE FRANK-READ SOURCE SEGMENT VERSUS SIMULATION TIME FOR DIFFERENT STRAIN RATES, SIMULATED WITH 3D-DDD. TIME REQUIRED FOR GENERATION OF THE THIRD LOOP FOR THE CASE OF ERATE=1E3 IS DENOTED BY T_3

In Figure 3-4 points with sudden decrease in the amount of net force are new loop generation instances and as expected, before generation of a loop there is a peak force corresponding to maximum line tension of semi-circle. As the simulation continues, stresses increase and as can be seen the amount of forces on the segment associated with loop generation increases. Also, time interval between generations of two loops decrease over time. Clearly, an approximate linear relationship can be seen for sum of the net force with respect to simulation time and the slope depends on the strain rate. To capture the loop generation mechanism in GPDDD, following steps are taken:

1. Values of source activation force and minimum time required for loop generation are assumed based on the strain rate and Figure 3-4.
2. At each step of the simulation, if the total amount of forces acting in the shear direction of the source, exceeds the source activation force, time criteria is checked. If the force is less than required amount, no loop is added at this time step.

3. If the forces are more than source activation force, and simulation time difference from the previous loop nucleation step is more than the minimum value, a loop is added around the source. If time is less than minimum value, no loop is added at this time step. Simulation continues until the simulation time is bigger than required value.
4. Amounts of source activation force is increase by 5% and minimum time interval is reduced to its 85% for next loop generation and the simulation is continued.

As can be seen in the Figure 3-4, net forces on the Frank-Read source increases over simulation and increment values decrease. Also, amount of time interval between nucleation of two consecutive loops decreases over time. This justifies increasing the values of source activation force and decreasing the minimum time interval in the above algorithm after nucleation of a loop. Figure 3-5 shows two different time steps of the GPDDD simulation of a single source corresponding to two values of strain as in Figure 3-4.

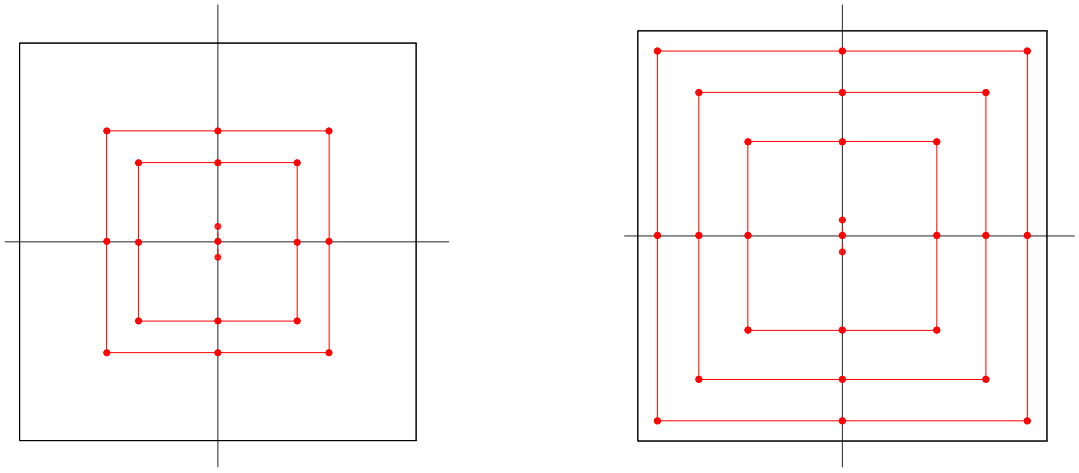

FIGURE 3-5. NUCLEATION OF LOOPS AROUND THE SOURCE IN GPDDD. UNLIKE 3D-DDD, BOWING OUT OF THE SOURCE SEGMENT IS NOT SIMULATED. (A) STRAIN=4.1E-4. (B) STRAIN=5.6E—4

The last remaining piece in simulating the Frank-Read source mechanism by adding rectangles around the source, is size of the added loops. To preserve the overall plastic strain of the system, size of the rectangles, are selected to be approximately equal to the loops generated with Frank-Read Source. So, in the 3D-DDD simulation of single Frank-Read source, area of the nucleated loop was calculated immediately after their generation and the values are as follows:

TABLE 3-2. VALUES OF AREA$^{1/2}$ OF THE LOOPS GENERATED BY A SINGLE 4 μm FRANK-READ SOURCE BASED ON 3D-DDD SIMULATION

eRate	1st loop	2nd loop	3rd loop	4th loop	5th loop
1e3	15.1	14	13	13.3	13.4
2e3	15.1	15.6	14.2	13.5	12.9
3e3	13.8	13	13	13.2	12.5
5e3	14.5	14.4	13	12.2	13

Based on these values an approximate size of 12 μm, which is three time the length of the source is selected for the sides of the new rectangles added around the loop.

The stress-strain curve for the case of eRate=1e3 is presented in Figure 3-6, comparing the two simulation types.

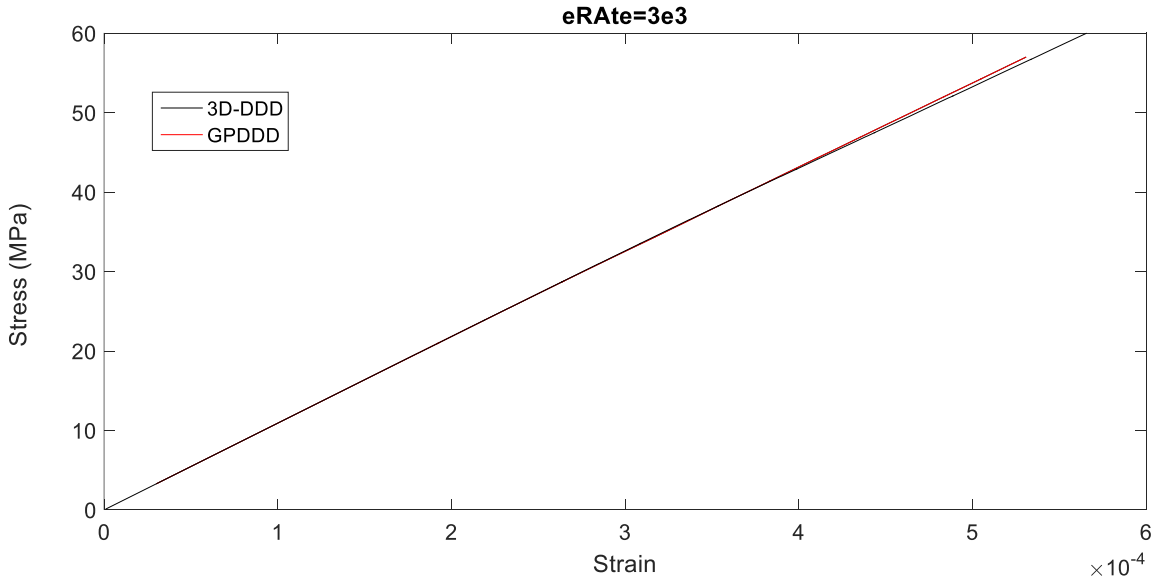

FIGURE 3-6. SHEAR STRESS- SHEAR STRAIN CURVE COMPARISON OF A SINGLE FRANK-READ SOURCE SIMULATED WITH 3D-DDD AND MATCHING IT WITH DISLOCATION SOURCE MECHANISM OF GPDDD.

It can be seen that by carefully selecting the values of source activation force and minimum time interval for a dislocation loop source, stress-strain curve corresponding to a Frank-Read source can be captured with an acceptable accuracy. Stress-strain curves corresponding to other values of

strain rate are similar to this case and are not presented to save space. Next, amounts of dislocation density is plotted against the strain of the system in Figure 3-7. Dislocation density is defined as the total length of the dislocations inside the simulation cell, divided by the volume of the cell and has the unit of m^{-2}.

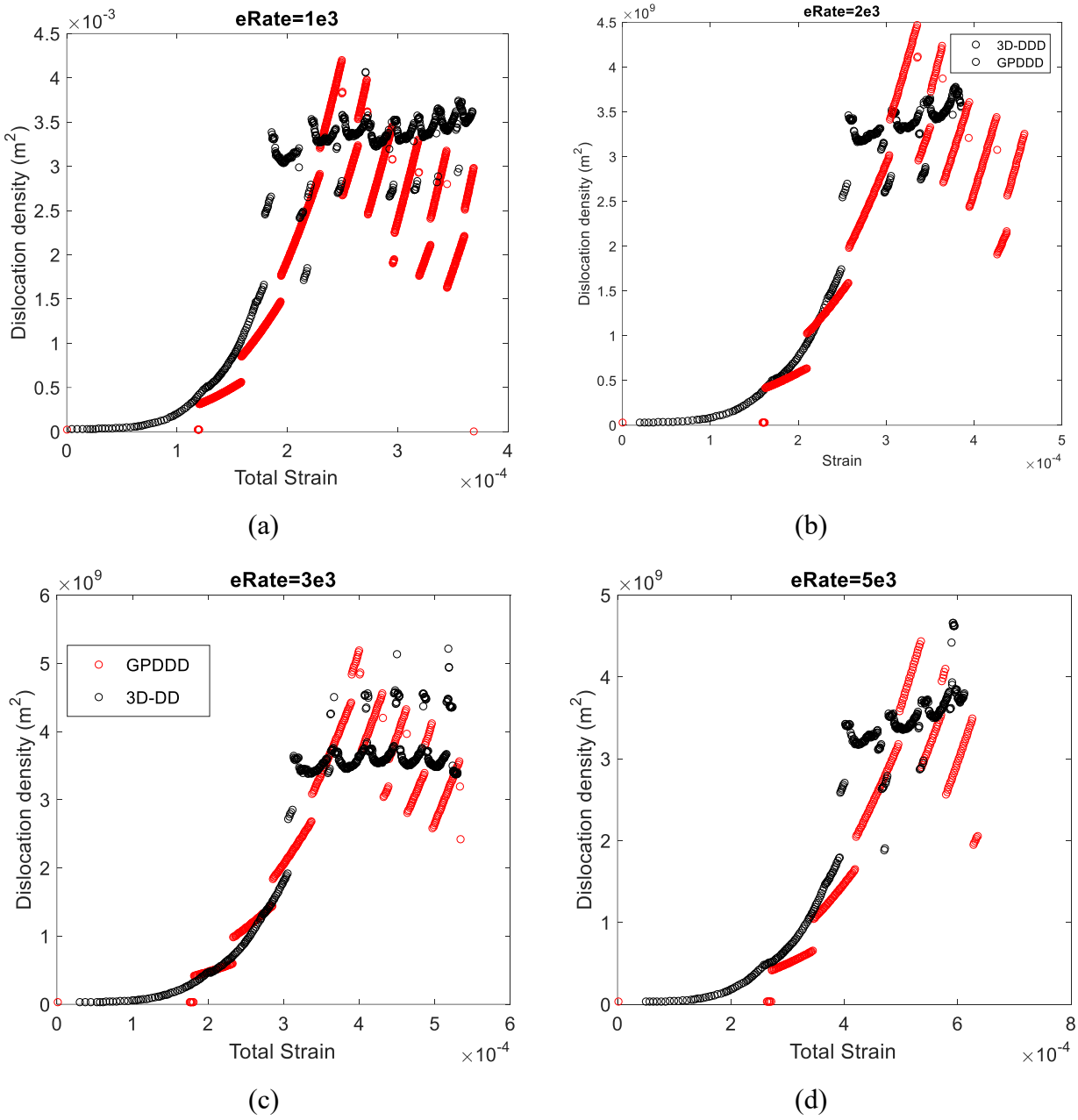

FIGURE 3-7. DISLOCATION DENSITY VS. SHEAR STRAIN OF A SINGLE PLANE CONTAINING SINGLE SOURCE, SIMULATED WITH 3D-DDD AND GPDDD USING DIFFERENT STRAIN RATES. RED AND BLACK MARKERS CORRESPONDS TO GPDDD AND 3D-DDD RESPECTIVELY.

It can be seen that there is a good level of consistency for the dislocation density corresponding to two methods. Lastly, the amount of forces on the dislocation source versus simulation time is plotted in Figure 3-8 and compared with the ones of 3D-DDD simulation.

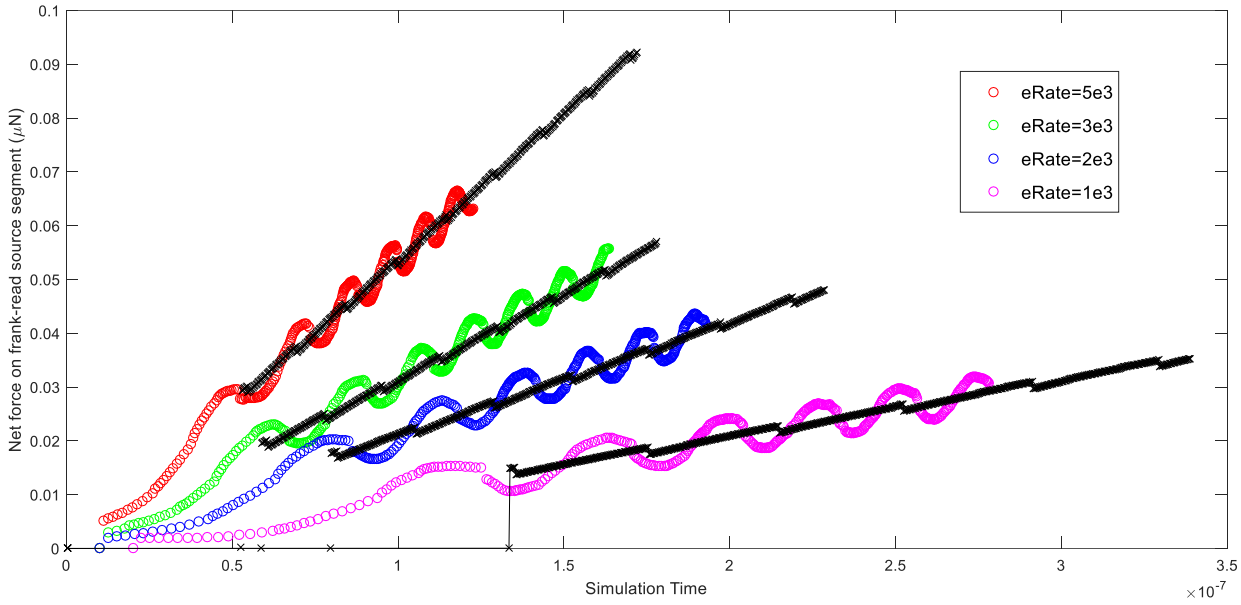

FIGURE 3-8. COMPARISON OF THE TOTAL FORCE ACTING ON THE FRANK-READ SEGMENT IN THE CASE OF SINGLE SOURCE, CALCULATED WITH GPDDD AND 3D-DDD USING DIFFERENT STRAIN RATES. BLACK MARKS CORRESPOND TO GPDDD AND COLORED ONES ARE FOR 3D-DDD.

Previously, it was mentioned one of the major advantages of the GPDDD is to simulate movement of dislocations with considerably less degrees of freedom which considerably reduces the computational cost. Plot of the wall time, which is the time required for the simulation to finish, versus shear strain for the two methods is presented in Figure 3-9. It can be seen that while the wall time of 3D-DDD increases exponentially versus shear strain, wall time of the GPDDD method has roughly linear relationship with shear strain.

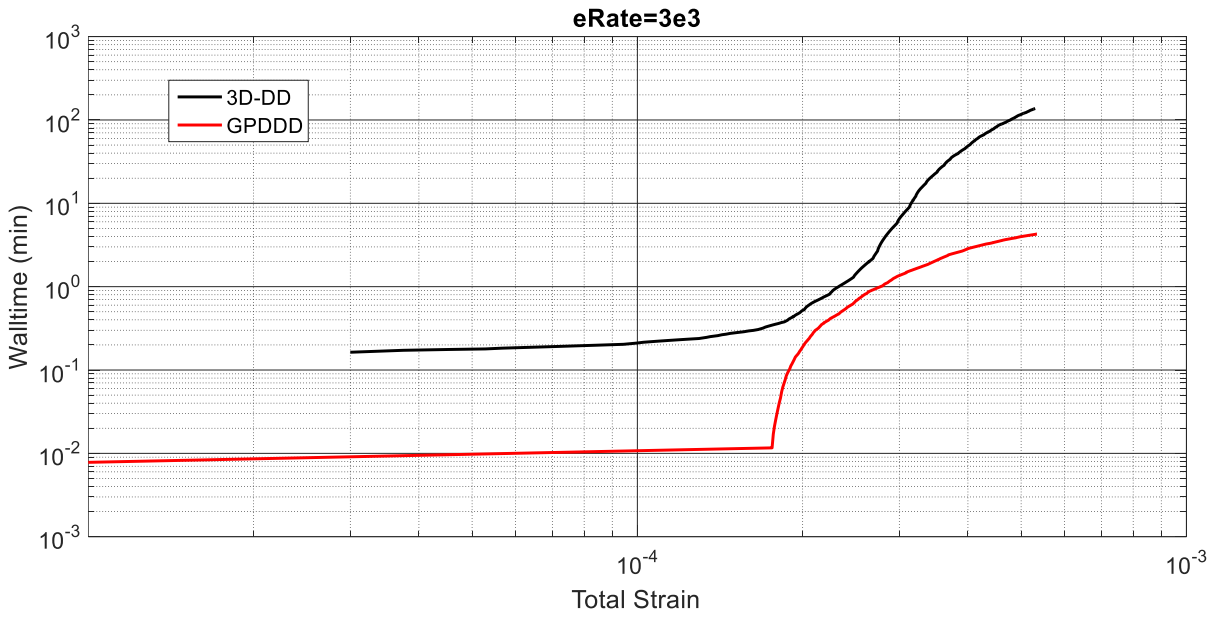

FIGURE 3-9. COMPARISON OF PROCESS TIME REQUIRED FOR THE SIMULATION OF A SINGLE FRANK-READ SOURCE TO COMPLETE. SIMULATIONS WERE PERFORMED ON HHPC CLUSTER.

Moreover, number of dislocation segments in the two methods are presented in the Figure 3-10. As mentioned in the section 2.1.1, process time required for calculation of node forces at each time step correlates with square of number of segments. Thus, by reducing the number of segments, process time of this step will be reduced.

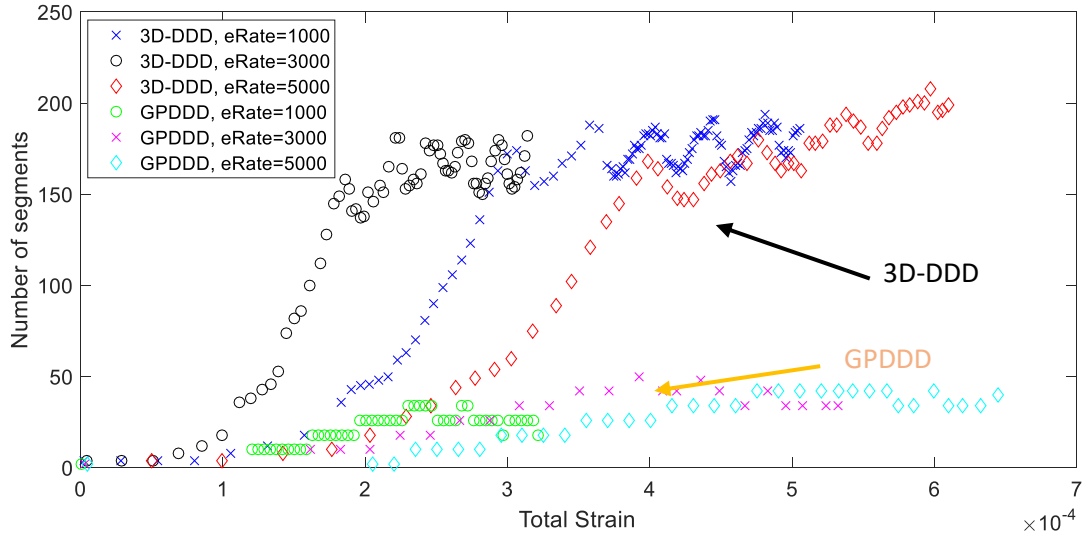

FIGURE 3-10. EVOLUTION OF NUMBER OF SEGMENTS DURING SIMULATION OF A SINGLE SOURCE USING 3D-DDD AND GPDDD FOR DIFFERENT VALUES OF STRAIN RATES.

Chapter 4

Single-slip loading of copper

4.1 Computational set up

All the simulations were done by modifying the MATLAB code, *DDLab*, such that rectangles were introduced as GPDDD shapes with all the associated shape transformations such as merging and collision with obstacles in accordance with the section 2.2. Periodic boundary conditions in all directions were used as explained in section 2.1.2.2. and long range forces were calculated based on pre-tabulated image stresses on a 2×2 grid. All the simulations were run in serial and Homewood High Performance Compute Cluster (HHPC) were used for all the wall times reported. Material properties used were that of copper as shown in Table 3-1 and the other simulation parameters are as follows:

TABLE 4-1.SIMULATION PARAMETERS

Property	Parameter	Value
Simulation cell size	L	50 μm
Collision radius	*rann*	1 μm
Maximum time step	*dt0*	2E-10 *sec*
Strain rate	*eRate*	5E2 – 5E3 s^{-1}
Minimum time delay between two loop	$Loop_{min(t)}$	1E-9 – 2E-9 *sec*

Five test cases were selected and for each one a parameter study was performed in which the influence of source activation force (SourceAF), obstacle strength (ObsStr), strain rate (eRate) and initial configuration of source and obstacles were examined via evolution of stress-strain curves. For all the simulations only one slip system is assumed to be active, thus cross slip and multiple slip systems are not considered. Simulation cell coordinates were selected different than crystallographic coordinates as [111], $[1\bar{1}0]$ and $[11\bar{2}]$ according to slip system of $[1\bar{1}0](111)$ as shown in the figure below. In this manner slip plane is the 2-3 plane and segments of a plane exiting the simulation cell, enter the cell from the opposing side on the same plane. This is not the case if simulation cell coordinates aligns with crystallographic directions.

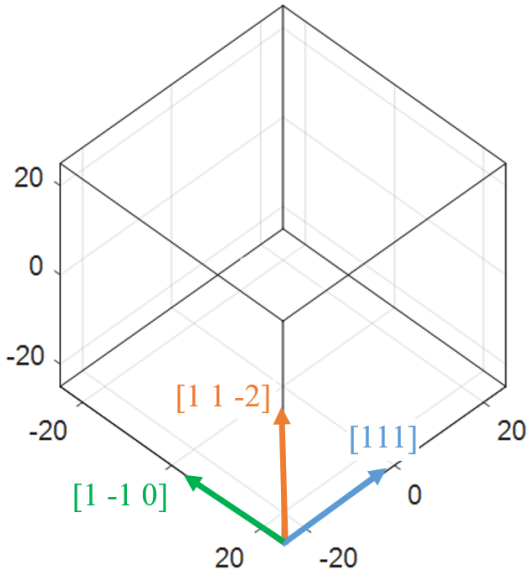

FIGURE 4-1. $50\times50\times50$ μm ***SIMULATION CELL AND ITS COORDINATES. COORDINATED WERE CHOSEN ACCORDING TO SLIP SYSTEM.***

Simulated test cases consist of sources and obstacles distributed in single-plane and multi-planes. For the case of single plane, four configurations are considered and they consist of two sources, symmetric one source and two obstacle and one source and four obstacles as shown in the Figure 4-2, Figure 4-5 and Figure 4-10, respectively. As for multi planes, simulation of 10 planes each containing one or two sources and four obstacles as shown in the Figure 4-16 and Figure 4-20 with randomly generated initial configurations is performed. Burgers vector of the sources and

obstacles, as well as all the added loops are the same and it aligns with negative direction of *x* axis based on the choice of coordinates as in Figure 4-1. Another issue to note is that time steps before nucleation of first loop are not simulated since they represent the linear part of the stress-strain curve. For this purpose, forces on each source is calculated at first step and at the second step, time interval *dt* is increased proportional to minimum value of source activation force over source forces. Amount of time step is reduced to *dt*0 after second step. Obtained results are presented in the next section, starting with single plane and followed by multi planes.

4.2 Single-plane results

4.2.1 Two sources

As a first example in this section, two Frank-Read sources on the same plane were considered and comparisons of walltime and dislocation density versus total strain are presented. Simulations were done assuming a strain rate of 2E+3 sec^{-1}. In the GPDDD method, activation force and minimum loop generation time interval of sources were tuned to the values obtained from DDD similar to Figure 3-8. Following figure compares the dislocation configuration of both methods at four time steps with equal shear strain.

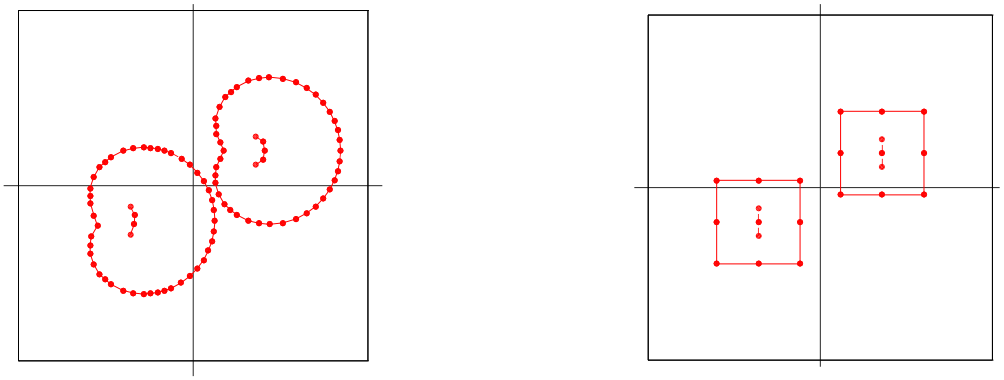

(a)

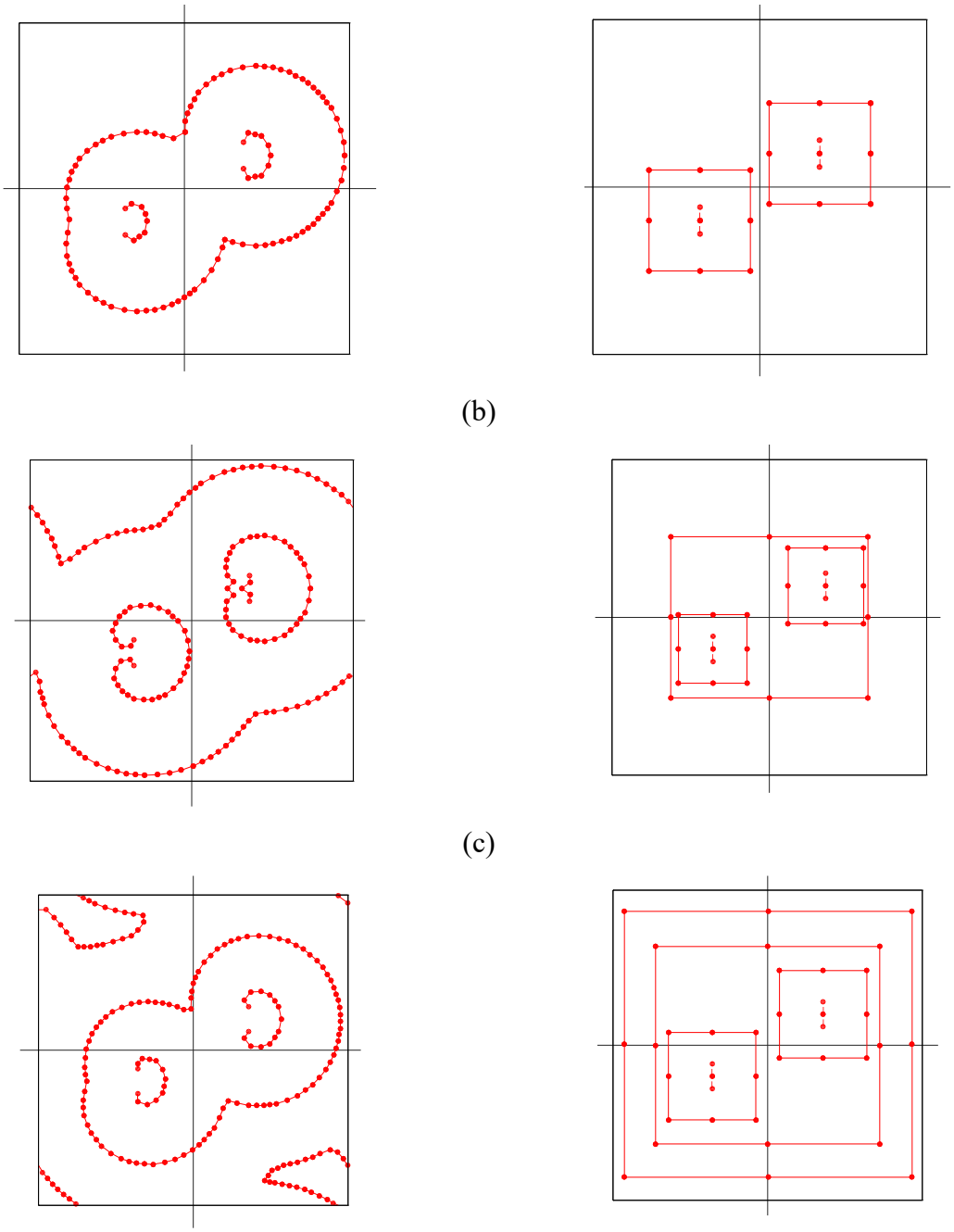

FIGURE 4-2. SIMULATION OF TWO SOURCES ON ONE PLANE USING DDD AND GPDDD. (A) STRAIN= $1.8E-4$***. (B) STRAIN=*** $2E-4$***. (C) STRAIN=*** $2.3E-4$***. (D) STRAIN=*** $3.4E-4$

Additional figures to compare both methods is presented below. It can be seen in Figure 4-3 that while GPDDD gives almost the same amount of dislocation density as DDD method during simulation, the total number of segments associated with GPDDD is considerably less than DDD.

At the point of dislocation saturation, DDD method consist of approximately 160 segments whereas corresponding value of GPDDD is less than 50 segments. This fact would result in significant reduction of the simulation time as depicted in Figure 4-4 from approximately 60 minutes for the DDD to less than 10 minutes.

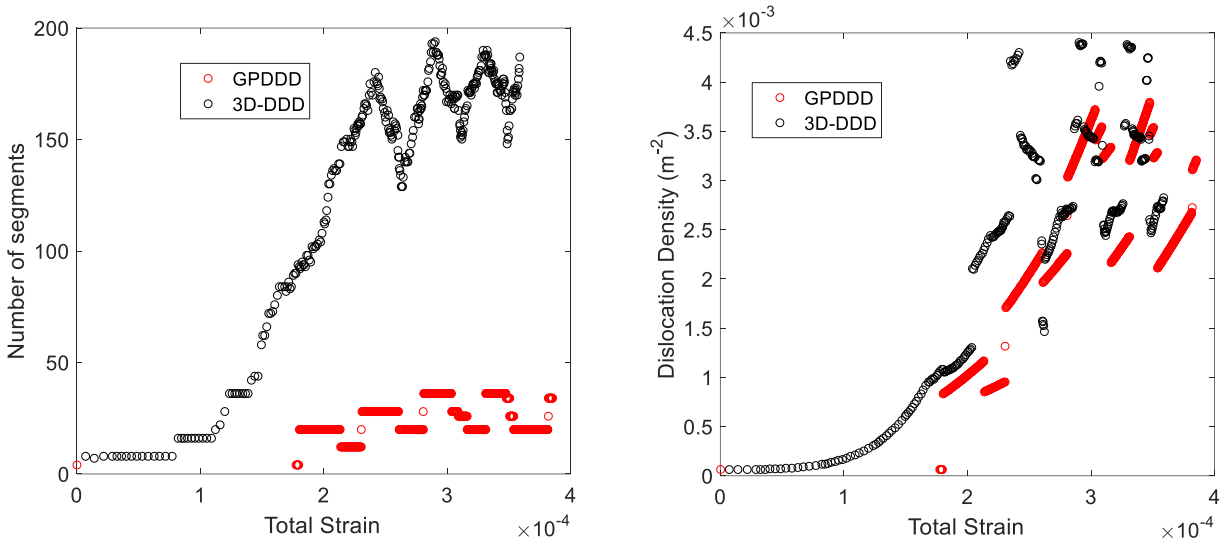

FIGURE 4-3. EVOLUTION OF DISLOCATION DENSITY AND TOTAL NUMBER OF SEGMENTS CORRESPONDING TO DDD AND GPDDD SIMULATION OF TWO SOURCES ON ONE PLANE.

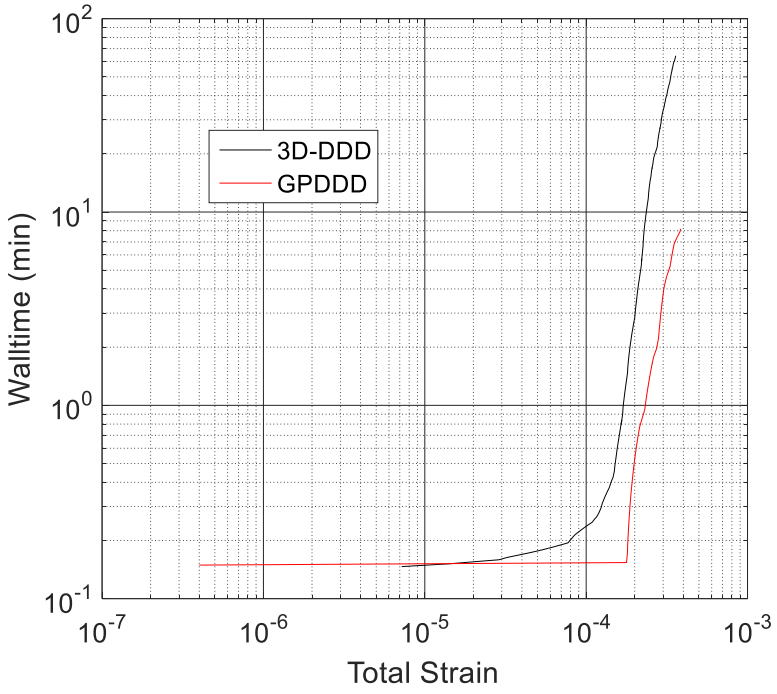

FIGURE 4-4. COMPARISON OF THE PROCESS TIME REQUIRED FOR THE SIMULATION OF TWO SOURCES ON ONE PLANE TO COMPLETE. SIMULATIONS WERE PERFORMED ON HHPC CLUSTER.

4.2.2 One source and two obstacles

Second configuration considered for the case of single plane includes one source and two obstacles on both sides of the source as shown in the figure below. GPDDD simulation were done for distances of 10 μm and 15 μm between source and obstacles which are denoted by configuration (I) and (II) respectively.

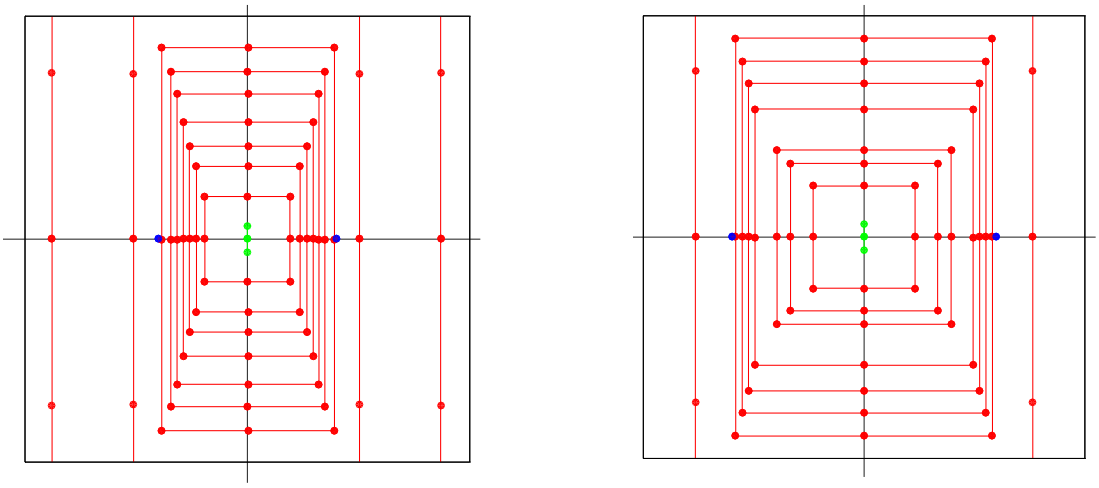

(a) (b)

FIGURE 4-5. LOCATION OF THE SOURCE AND OBSTACLES RELATIVE TO EACH OTHER. SOURCES ARE SHOWN BY GREEN DOTS AND OBSTACCLES AS BLUE WHILE MOBILE DISLOCATION SEGMENTS ARE SHOWN BY RED. DISTANCE BETWEEN THE SOURCE AND OBSTACLES ARE (A) 10 μm ***, CONFIGURATION (***I***) . (B)*** 15 μm ***, CONFIGURATION (***II***)***

Minimum distance between segments as explained in section 2.2.3.2 can be observed in Figure 4-5. Simulations were performed for 16 combinations of different values for source activation force and obstacle strength subjected to strain rate of 1E+3 and 3E+3. Stress-strain curves are shown in the figures below.

It can be seen from all the four curves that increasing activation force, results in higher values of stress corresponding to nonlinearity start. In other words, activation force has direct correlation with yield stress of crystal. Moreover, the stronger are the obstacles, the more is the strain hardening. This fact is due to influence of obstacles on locking dislocation and suddenly releasing them, which requires higher stresses for dislocations to pass obstacles and reach the same amount of strain increment.

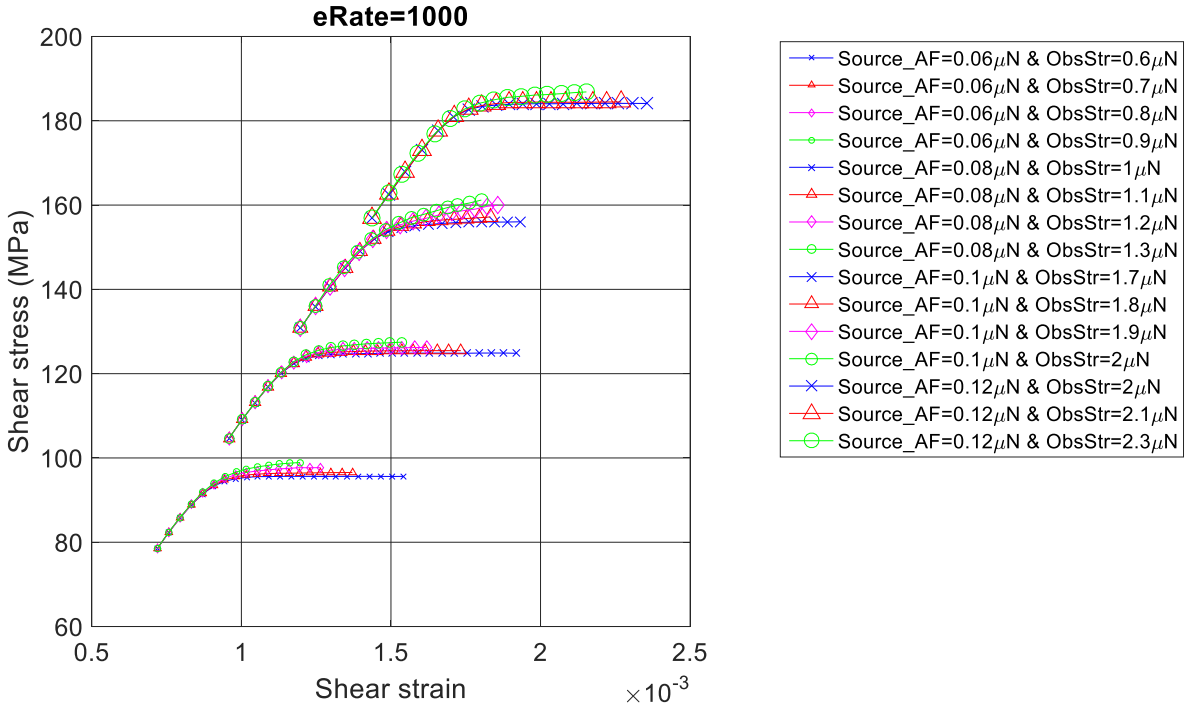

FIGURE 4-6. STRESS-STRAIN CURVES OF 16 COMBINATIONS OF SOURCE ACTIVATION FORCE AND OBSTACLE STRENGTH SUBJECTED TO STRAIN RATE OF 1000 CORRESPONDING TO CONFIGURATION (I) WITH ONE SOURCE AND TWO OBSTACLES ON ONE PLANE. LARGER MARKER SIZE CORRESPONDS TO LARGER ACTIVATION FORCE, WHICH VARIES FROM 0.06 μN TO 0.12 μN .

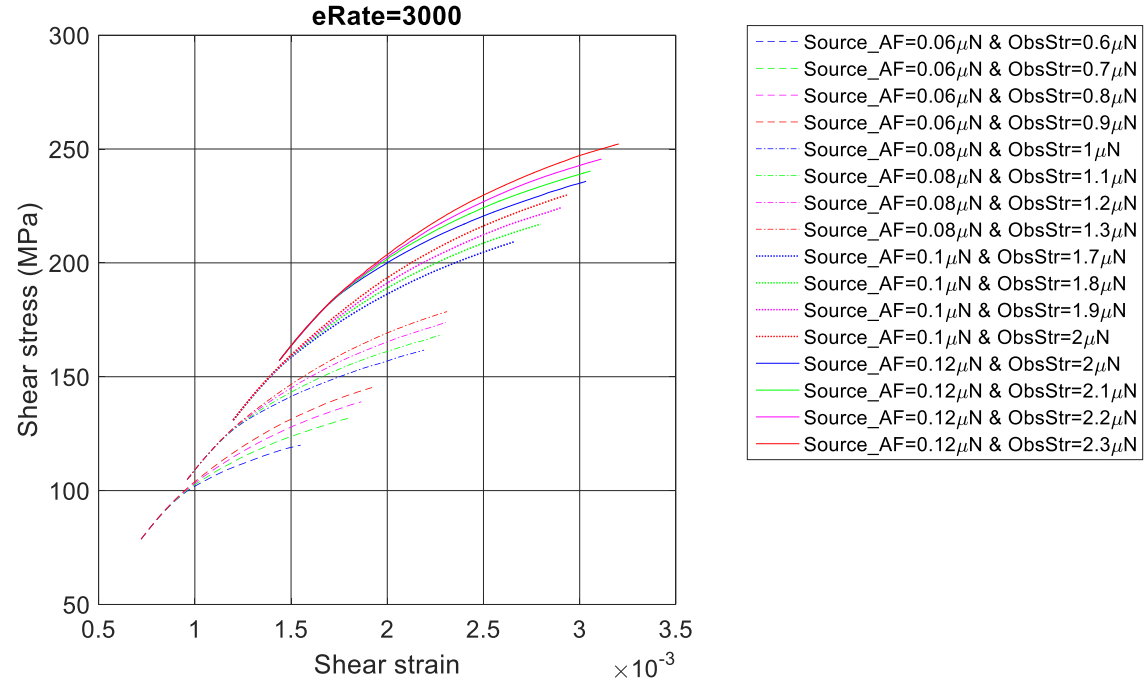

FIGURE 4-7. STRESS-STRAIN CURVES OF 16 COMBINATIONS OF SOURCE ACTIVATION FORCE AND OBSTACLE STRENGTH SUBJECTED TO STRAIN RATE OF 3000 CORRESPONDING TO CONFIGURATION (I) WITH ONE SOURCE AND TWO OBSTACLES ON ONE PLANE

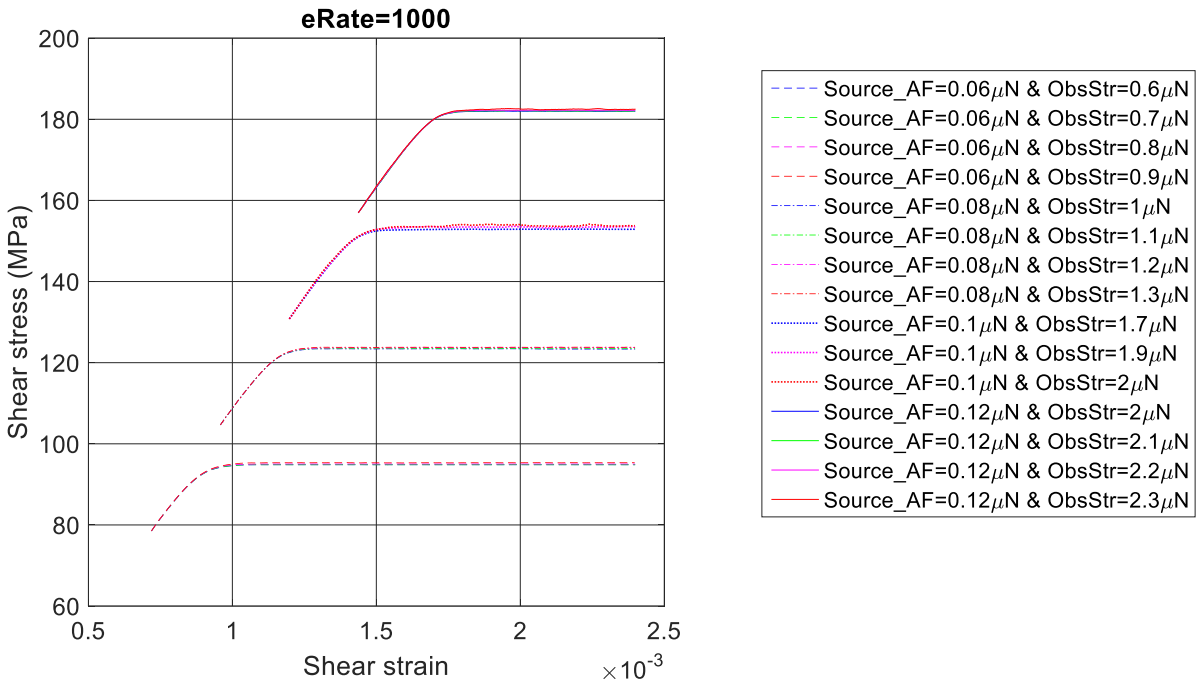

FIGURE 4-8. STRESS-STRAIN CURVES OF 16 COMBINATIONS OF SOURCE ACTIVATION FORCE AND OBSTACLE STRENGTH SUBJECTED TO STRAIN RATE OF 1000 CORRESPONDING TO CONFIGURATION (II) WITH ONE SOURCE AND TWO OBSTACLES ON ONE PLANE

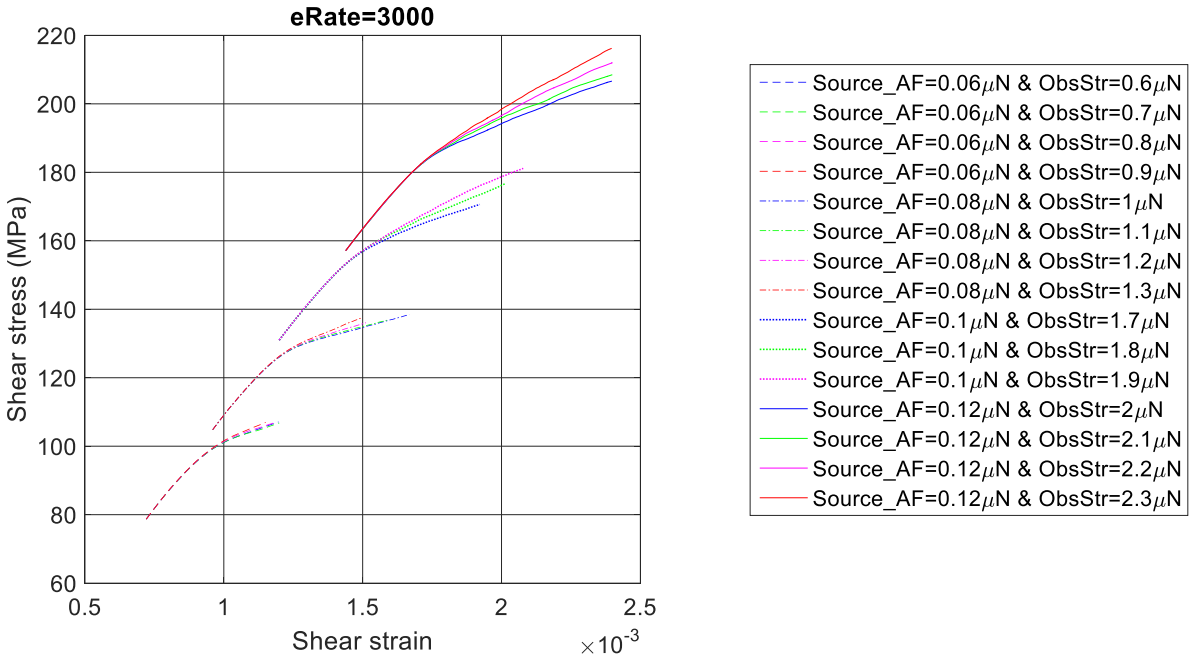

FIGURE 4-9. STRESS-STRAIN CURVES OF 16 COMBINATIONS OF SOURCE ACTIVATION FORCE AND OBSTACLE STRENGTH SUBJECTED TO STRAIN RATE OF 3000 CORRESPONDING TO CONFIGURATION (II) WITH ONE SOURCE AND TWO OBSTACLES ON ONE PLANE

The effect of obstacle strength in configuration (II) is not as significant as in configuration (I), which indicated that closer obstacles to the source play more significant role in the work hardening. This can be attributed to the fact that dislocation loops need more time to touch further obstacles than closer ones and as time increases, stresses increase too. Thus, forces on the segments touching the further obstacles are higher due to higher stresses. Moreover, the effect of increasing strain rate on both cases is more work hardening and higher stresses corresponding to start of nonlinearity in stress-strain curve. It must be noted that variation of elastic moduli with strain rate was ignored and constant values were assumed as shown in the Table 3-1.

4.2.3 One source and four obstacles

As a second case for single plane problems, one source and four obstacles were distributed in two different configurations denoted by (I) and (II) as shown in the following figure.

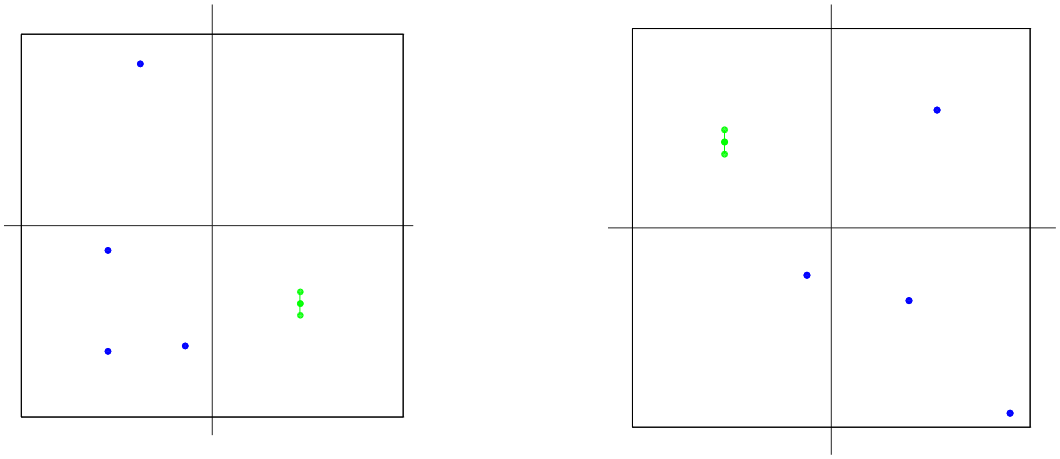

FIGURE 4-10. RANDOMLY SELECTED INITIAL CONFIGRATION OF SOURCE AND OBSTACELS. SOURCES ARE SHOWN BY GREEN DOTS AND OBSTACCLES AS BLUE (A) CONFIGURATION (I) (B) CONFIGUREATIO (II)

During simulations, loops are added around the source and they expand at each time step. Next, segments collide with obstacles, and their motion is hindered until the forces overcome the obstacle strength as explained in the section 2.2.3.1. Loops may self collide before or after passing the obstacle and completely annihilate or form line dislocations of edge (Figure 4-11(a)) or screw

(Figure 4-11(d)) character. Line dislocation can subsequently collide at an obstacle and stop until the force exceeds the strength of obstacle. Snapshots of two steps of simulation for each of the configurations is presented in the following figure.

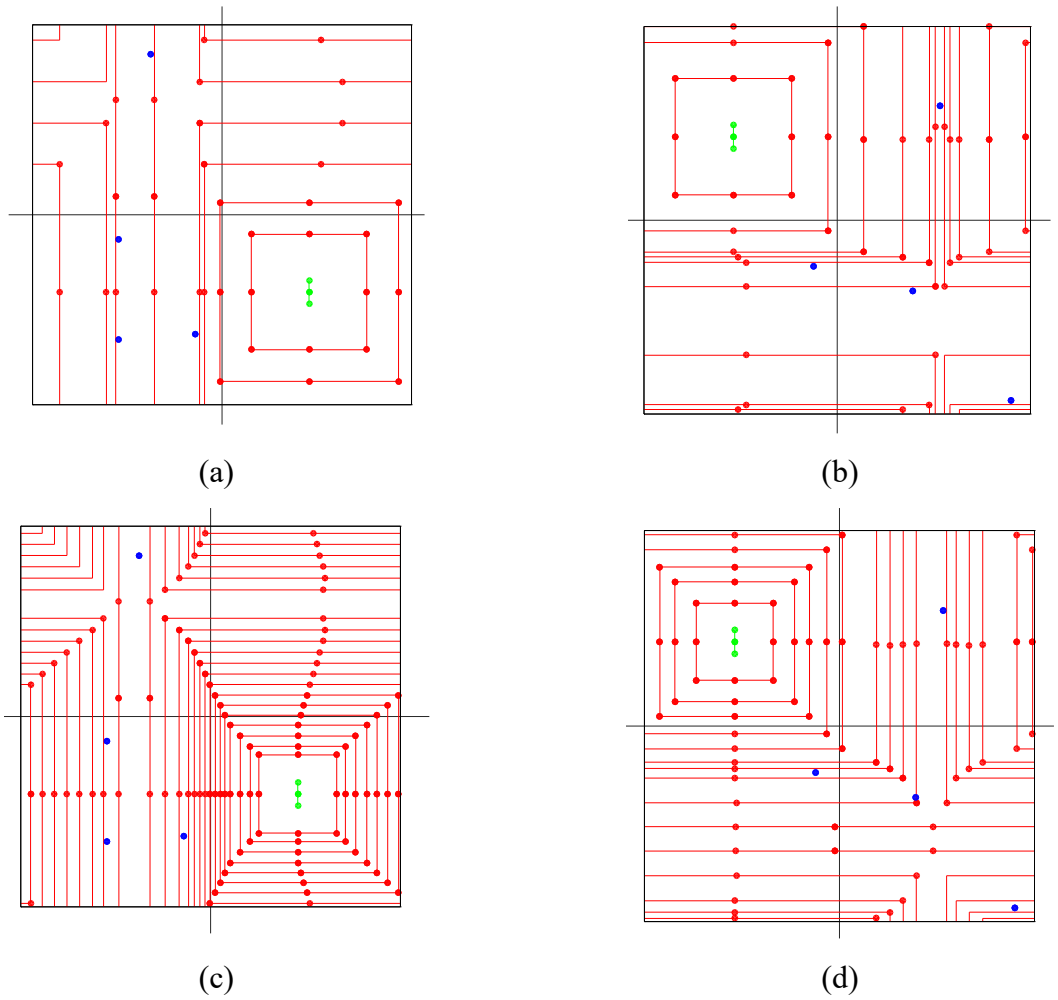

FIGURE 4-11. SNAPSHOTS OF SIMULATION AT TWO DIFFERENT TIME STEP. SOURCES ARE SHOWN BY GREEN DOTS AND OBSTACCLES AS BLUE WHILE DISLOCATION SEGMENTS ARE SHOWN BY RED. (A,C) CONFIGURATION (I) (B,D) CONFIGURATION (II)

Similar to the previous case, 16 different combinations for source activation force and obstacle strength were selected which are less than the values of previous section to make the yield stress closer to actual values. Results are presented in the following figures in an order similar to the previous section.

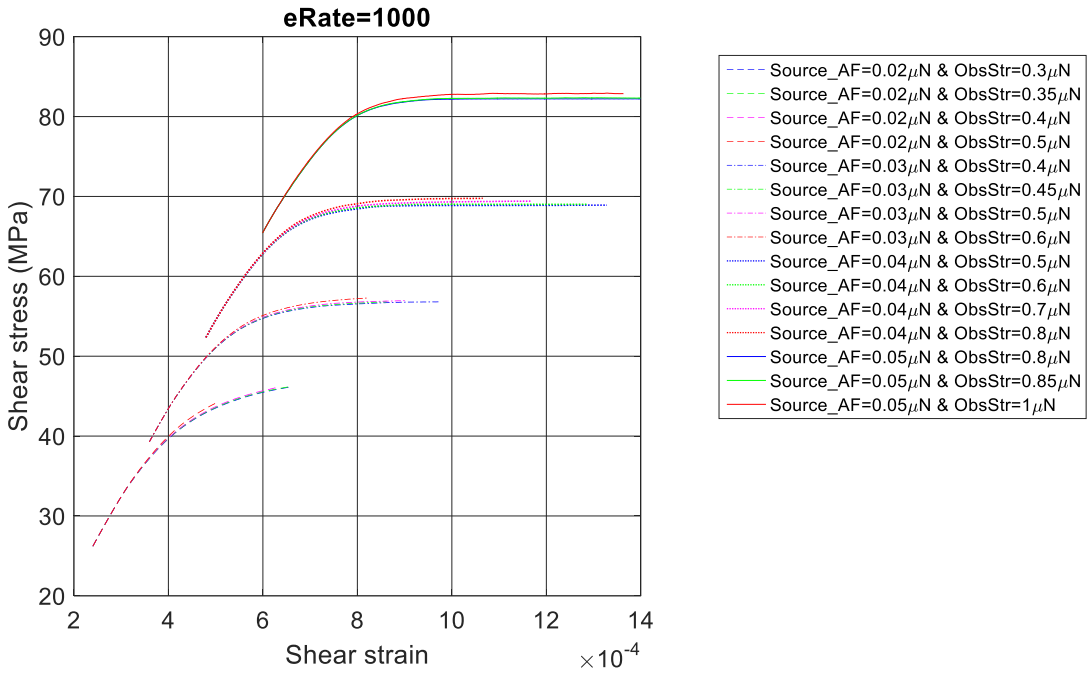

FIGURE 4-12. STRESS-STRAIN CURVES OF 16 COMBINATIONS OF SOURCE ACTIVATION FORCE AND OBSTACLE STRENGTH SUBJECTED TO STRAIN RATE OF 1000 CORRESPONDING TO CONFIGURATION (I) WITH ONE SOURCE AND FOUR OBSTACLES ON ONE PLANE

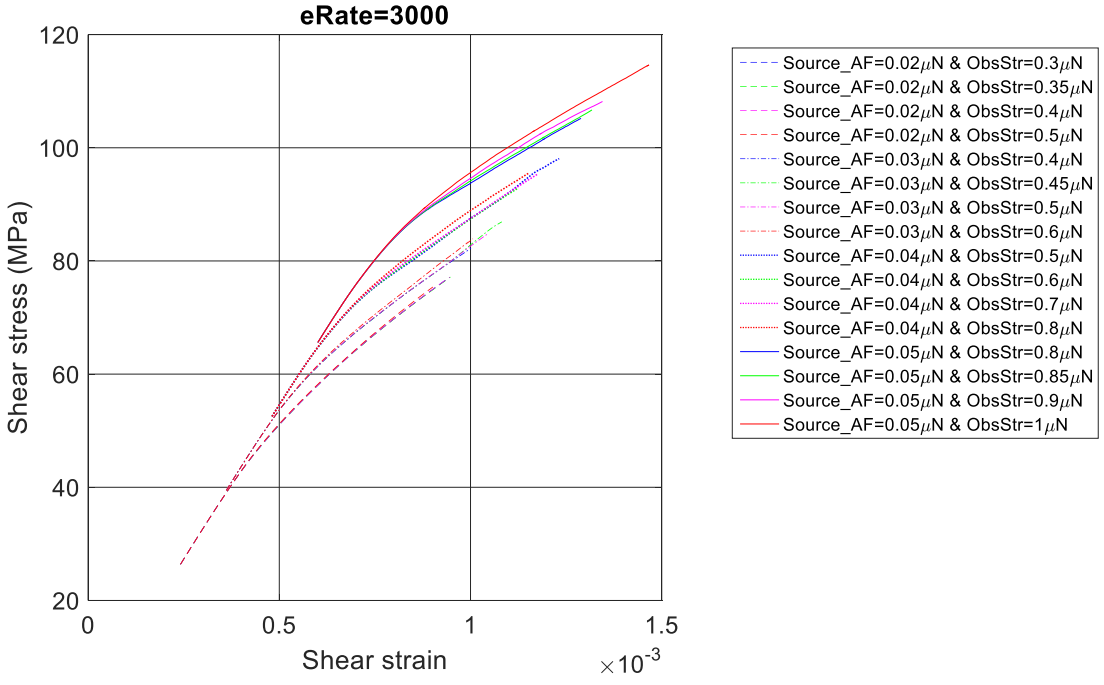

FIGURE 4-13. STRESS-STRAIN CURVES OF 16 COMBINATIONS OF SOURCE ACTIVATION FORCE AND OBSTACLE STRENGTH SUBJECTED TO STRAIN RATE OF 3000 CORRESPONDING TO CONFIGURATION (I) WITH ONE SOURCE AND FOUR OBSTACLES ON ONE PLANE

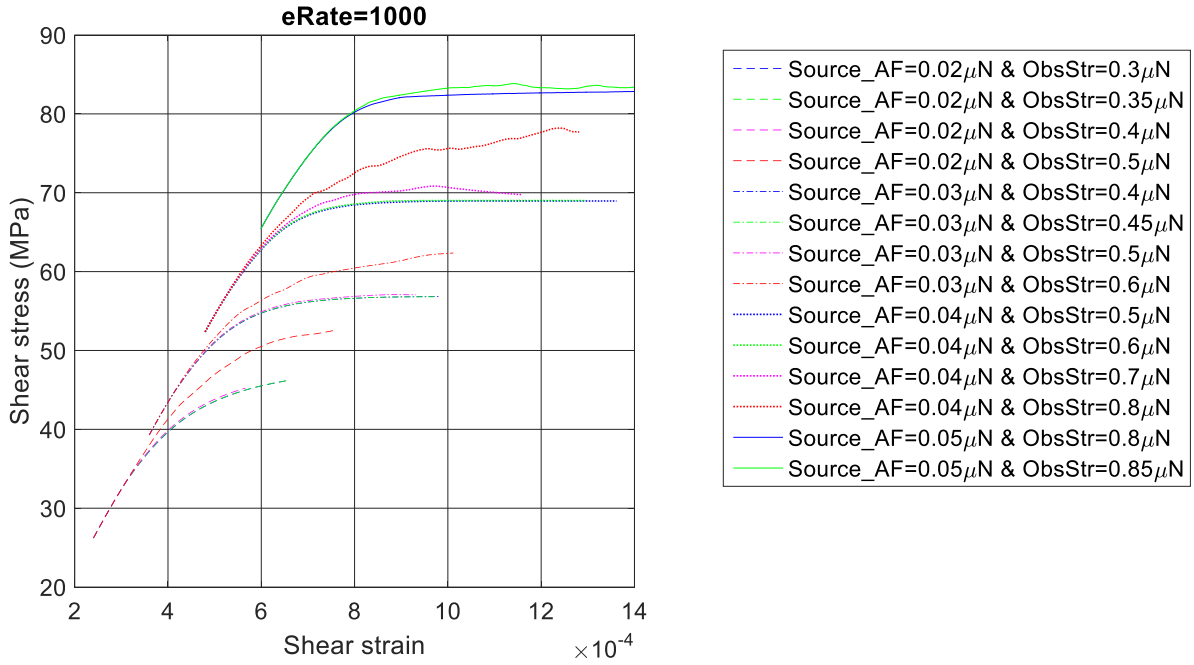

FIGURE 4-14. STRESS-STRAIN CURVES OF 16 COMBINATIONS OF SOURCE ACTIVATION FORCE AND OBSTACLE STRENGTH SUBJECTED TO STRAIN RATE OF 1000 CORRESPONDING TO CONFIGURATION (II) WITH ONE SOURCE AND FOUR OBSTACLES ON ONE PLANE

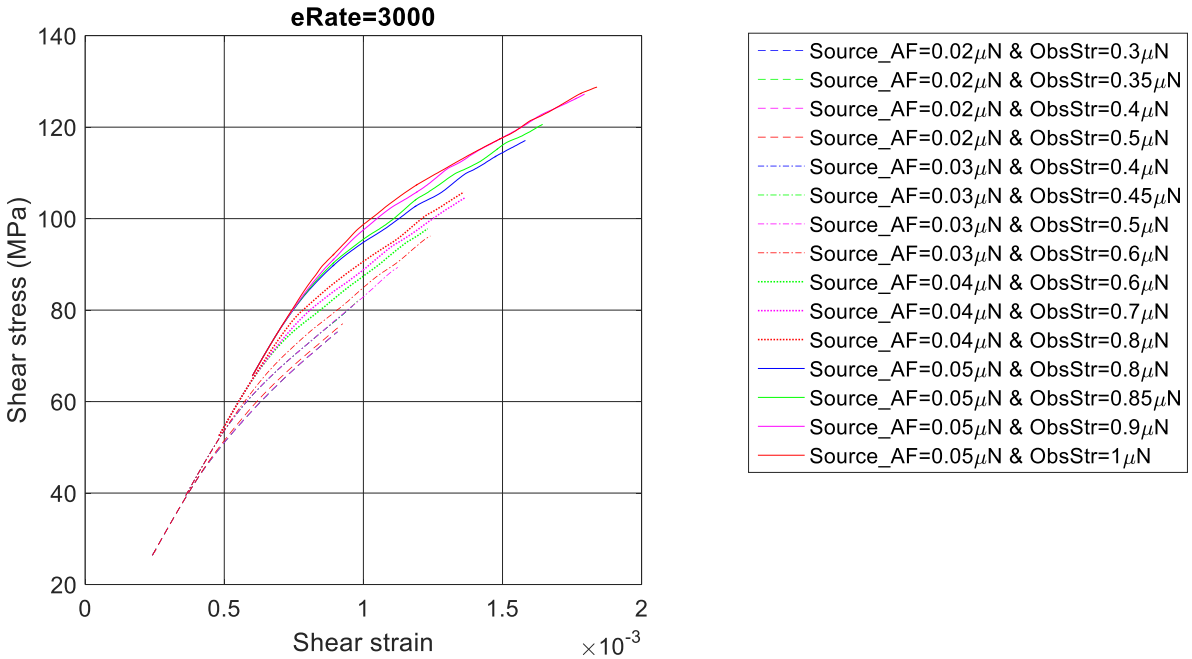

FIGURE 4-15. STRESS-STRAIN CURVES OF 16 COMBINATIONS OF SOURCE ACTIVATION FORCE AND OBSTACLE STRENGTH SUBJECTED TO STRAIN RATE OF 3000 CORRESPONDING TO CONFIGURATION (II) WITH ONE SOURCE AND FOUR OBSTACLES ON ONE PLANE

All the observations of the previous section, such as higher yield stress for higher activation force and more work hardening for higher obstacle strength can also be seen in this case.

4.3 Multi-plane results

As examples of large simulations, 10 slip planes in the same slip system were considered where each one contains four obstacles and one or two sources. First the case with one source at each plane is considered, then the case of two sources is presented.

4.3.1 Ten planes each containing one source and four obstacles

Ten parallel planes were selected inside the simulation cell and on each plane, one source were distributed as shown in Figure 4-16. Sources were distributed randomly provided that they are at least 8 μm (twice the size of the source) away from the cell's boundary. The reason for this choice is to have new loops added around the source, completely fall inside the cell, which otherwise would be partially inside the cell and partially on the other side of the cell, through applying periodic boundary conditions.

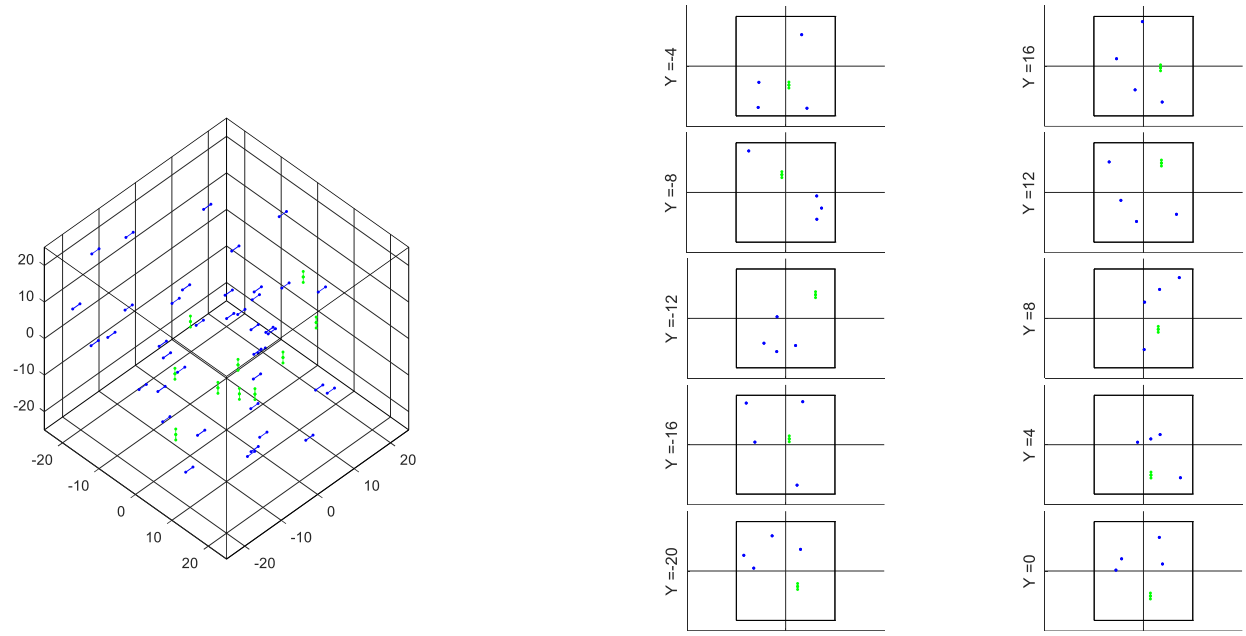

FIGURE 4-16. RANDOMLY SELECTED INITIAL CONFIGRATION OF SOURCE AND OBSTACELS IN THE SIMULATION CELL AND ON EACH PLANE. SOURCES ARE SHOWN BY GREEN DOTS AND OBSTACCLES AS BLUE

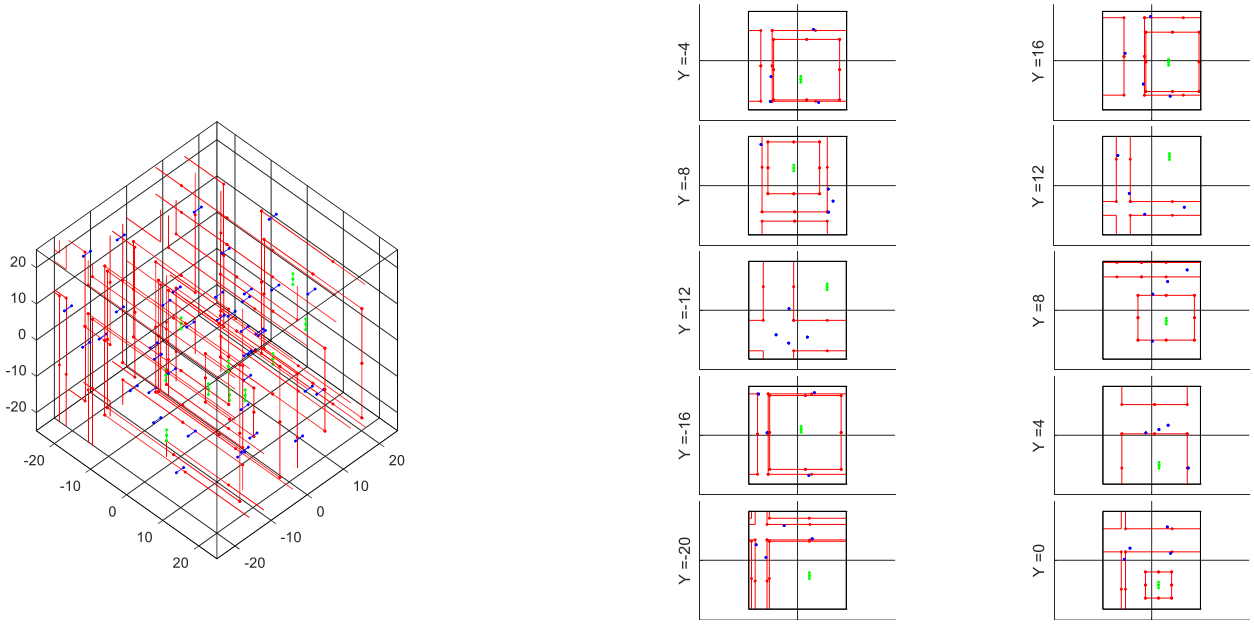

FIGURE 4-17. SIMULATION SNAPSHOT OF SINGLE SLIP LOADING OF COPPER WITH TEN PLANES, EACH CONTAINING ONE SOURCE AND FOUR OBSTACLES. SNAPSHOT CORRESPONDS TO STRAIN OF 6.5E-4

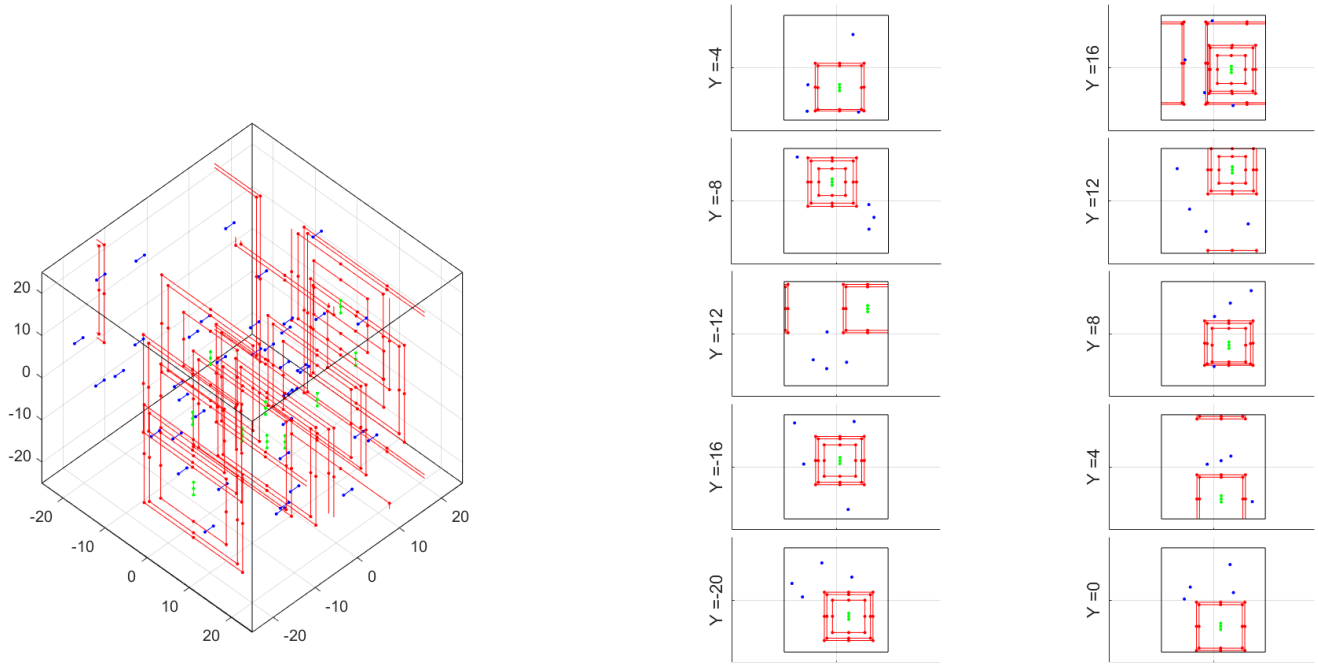

FIGURE 4-18 SIMULATION SNAPSHOT OF SINGLE SLIP LOADING OF COPPER WITH TEN PLANES, EACH CONTAINING ONE SOURCE AND FOUR OBSTACLES. SNAPSHOT CORRESPONDS TO STRAIN OF 7.6E-4

Initial source and obstacle distribution is shown in Figure 4-16, followed by presentation of two snapshots of simulation. Dislocation segments on different planes, interact with each other and impose forces on one another, which would lead to stress-strain curves different from those of individual planes. Figure 4-19 shows the stress-strain curves corresponding to 8 different combination of source activation force and obstacle strength. Each curve represent a separate simulation and all the simulations were running for 24 hours. One issue to notice in this figure is the slight fluctuations in stress values, which did not occur in the case of single plane.

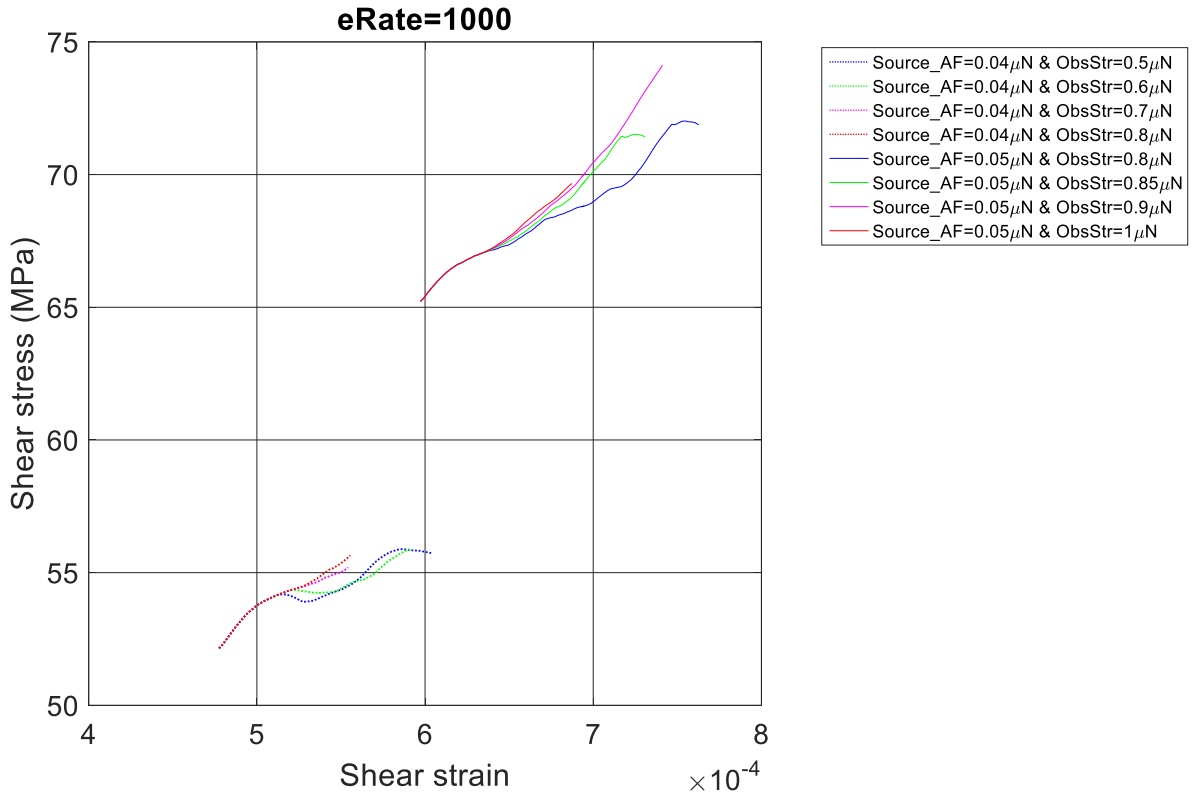

FIGURE 4-19. STRESS-STRAIN CURVES OF 8 COMBINATIONS OF SOURCE ACTIVATION FORCE AND OBSTACLE STRENGTH SUBJECTED TO STRAIN RATE OF 1000 CORRESPONDING TO CONFIGURATION SHOWN IN FIGURE 4-16

4.3.2 Ten planes each containing two sources and four obstacles

To show the efficiency of the algorithm developed for handling loop merging, which was described at section 2.2.3.2, large-size simulation was performed with ten planes, each containing two sources and four obstacles. Initial distribution of sources and obstacles in simulation cell and on each plane is shown on the Figure 4-20.

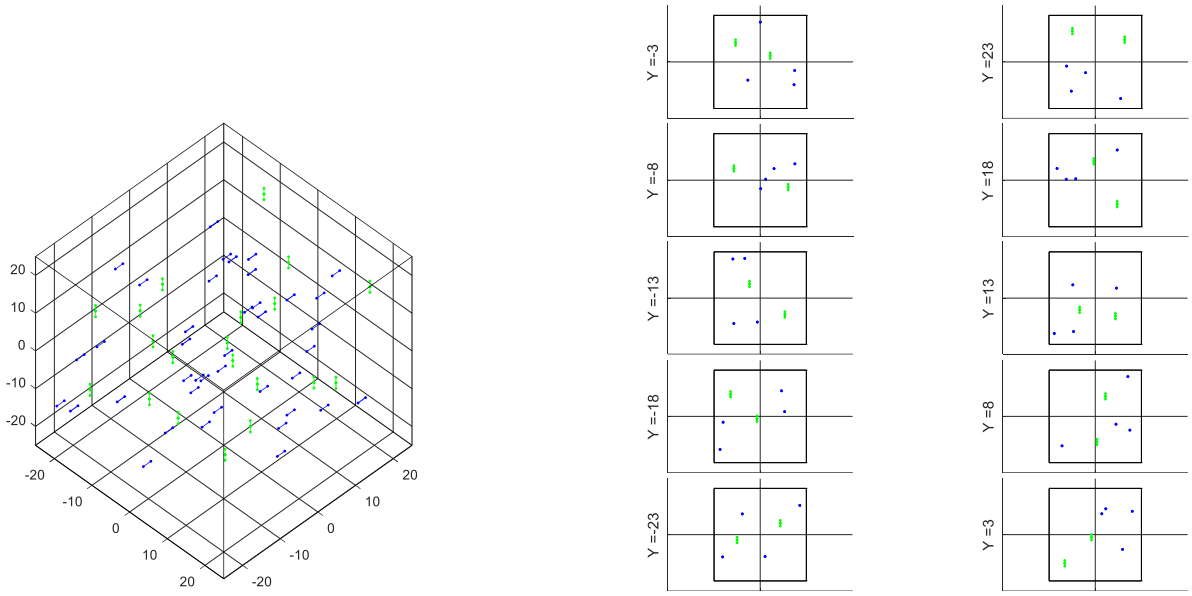

FIGURE 4-20. RANDOMLY SELECTED INITIAL CONFIGRATION SOURCE AND OBSTACELS IN THE SIMULATION CELL AND ON EACH PLANE. SOURCES ARE SHOWN BY GREEN DOTS AND OBSTACCLES AS BLUE

Number of initial dislocation segments for this case is 80 (4 source segments and 4 obstacle segments on each plane), which would result in considerably higher processor time as compared with single plane examples. This is because the most time consuming step of the DDD simulation is calculation of forces, which correlates with N^2 , with N being number of segments. However, still the processor time of GPDDD is much less than 3D-DDD. In fact stress-strain curves shown in Figure 4-23 were obtained by running the code for 24 hours. Simulation of this size using 3D-DDD would take weeks to complete.

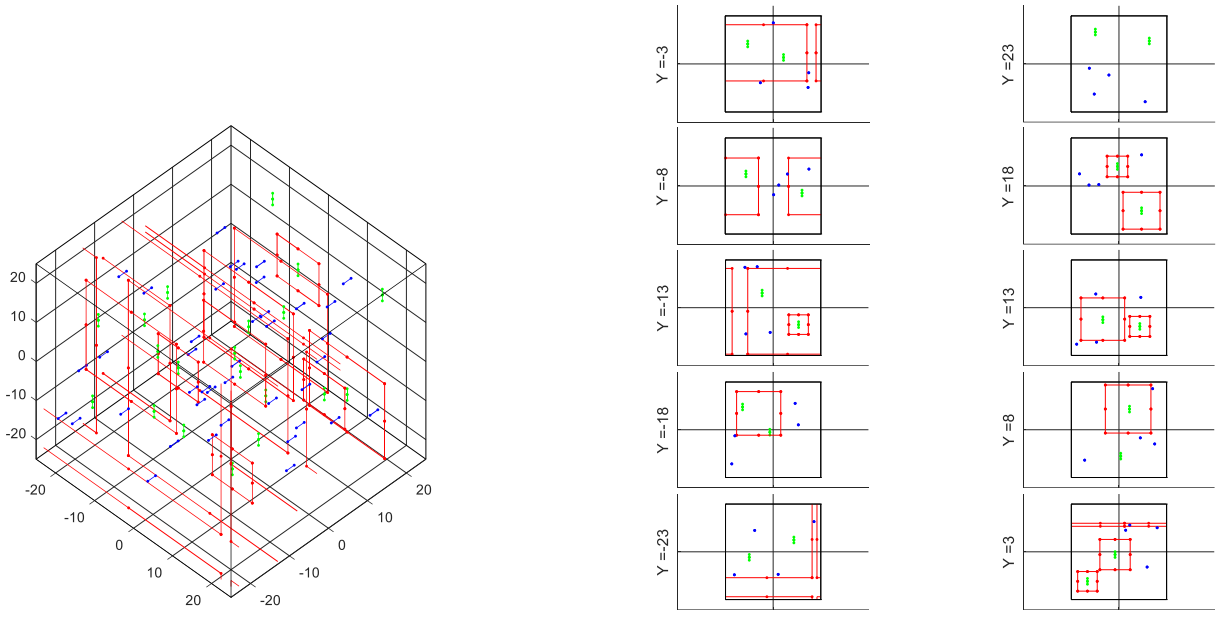

FIGURE 4-21. SIMULATION SNAPSHOT OF SINGLE SLIP LOADING OF COPPER WITH TEN PLANES, EACH CONTAINING TWO SOURCES AND FOUR OBSTACLES. SNAPSHOT CORRESPONDS TO STRAIN OF 7.3E-4

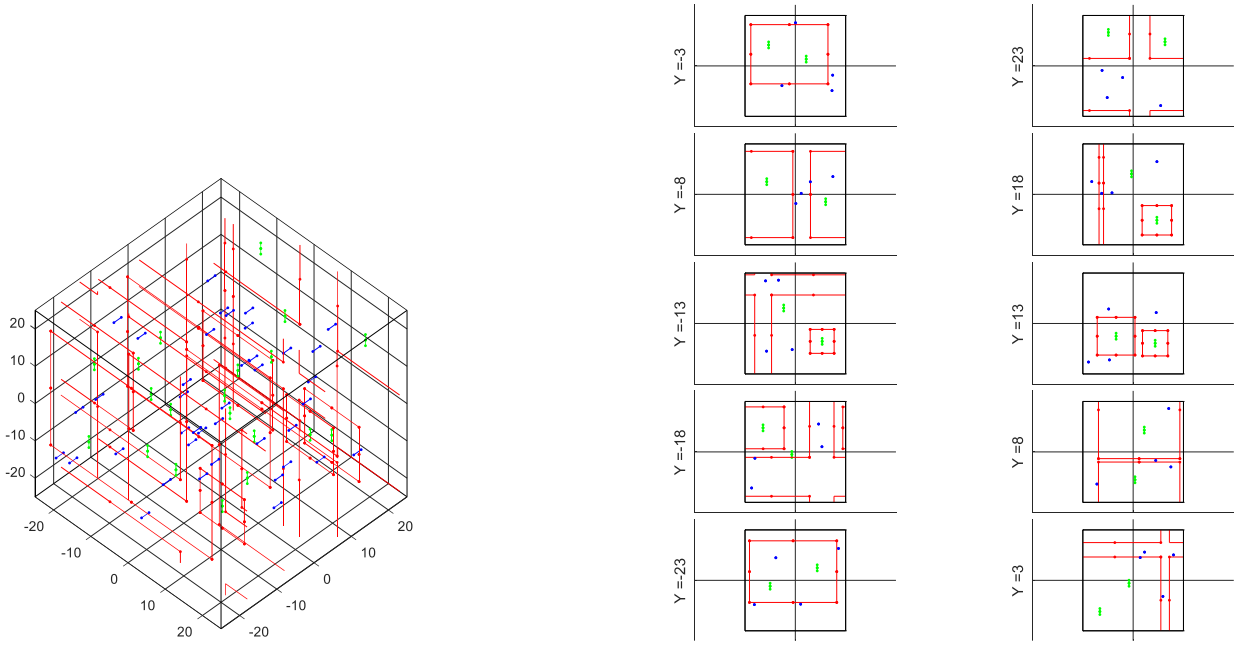

FIGURE 4-22. SIMULATION SNAPSHOT OF SINGLE SLIP LOADING OF COPPER WITH TEN PLANES, EACH CONTAINING TWO SOURCES AND FOUR OBSTACLES. SNAPSHOT CORRESPONDS TO STRAIN OF 8.7E-4

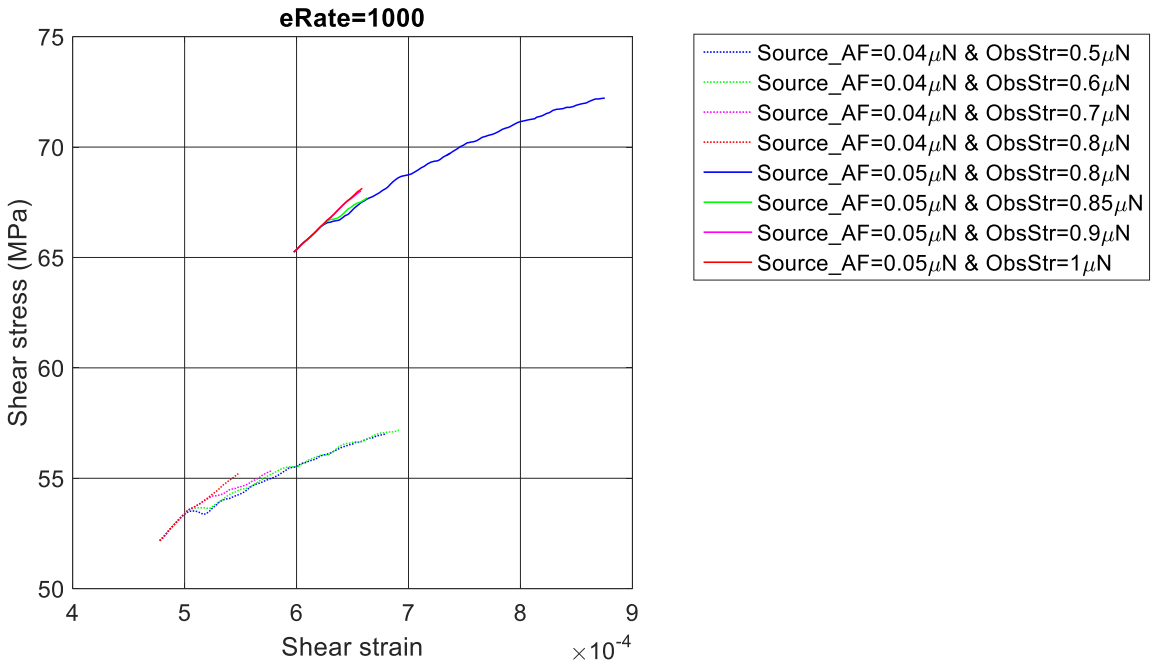

FIGURE 4-23. STRESS-STRAIN CURVES OF 8 COMBINATIONS OF SOURCE ACTIVATION FORCE AND OBSTACLE STRENGTH SUBJECTED TO STRAIN RATE OF 1000 CORRESPONDING TO CONFIGURATION SHOWN IN FIGURE 4-20.

Shamseddin(Hamed) Akhondzadeh

Akhondzadeh@gmail.com

EDUCATION

Stanford University Palo Alto, CA
PhD student in Mechanical Engineering
Adviser: Prof. Wei Cai

Johns Hopkins University Baltimore, MD
MSE in Civil Engineering August 2016
Research Adviser: Prof. Stefanos Papanikolaou; Academic Adviser: Prof. Lori Graham-Brady
MS Thesis title: "Geometrically projected discrete dislocation dynamics"

Sharif University of Technology Tehran, Iran
Master of Science in Structural Engineering January 2015
Adviser: Prof. Amir Reza Khoei
Thesis title: "Numerical simulation of stress singularities in multi-material media using the X-FEM"

K.N.Toosi University of Technology (KNTU) Tehran, Iran
Bachelor of Science in Civil Engineering June 2012

University of Isfahan Isfahan, Iran
Civil Engineering, Transferred to KNTU 2007 –2008

RESEARCH EXPERIENCE

Geometrically Projected Discrete Dislocation Dynamics
Johns Hopkins University, adviser: Prof. Stefanos Papanikolaou
In collaboration with Prof. Wei Cai, Prof. Erik Vandergiessen and Dr. Ryan Sills
Developing codes based on the open source code, DDLab, to simulate dislocation loops using a reduced order model

Nanoindentation of Micrograin in Polycrystals Under Multiaxial Stress
Johns Hopkins University, adviser: Prof. Stefanos Papanikolaou
Involved in EBSD and nanoindentation tests on copper samples and analyzing data to identify abrupt plastic yielding points (so-called pop-in behavior)

Numerical Simulation of Stress Singularities and Crack Propagation Path in Composite Materials, Sharif University of Technology, adviser: Prof. Amir Reza Khoei

- Introduced a new approach to simulate stress singularities using X-FEM and based on this new approach, parallel codes were developed from scratch to investigate stress singularities arising at crack tips terminating at bimaterial interfaces and multi-material junctions
- Investigated the problem of crack/hydraulic fracture propagation in the vicinity of material interfaces

References

1. Hull, Derek, and David J. Bacon. Introduction to dislocations. Vol. 37. Elsevier, 2011.

2. W. D. Nix, Partial dislocation tutorial for FCC metals. Stanford University.

3. Sills, Ryan B., and Wei Cai. "Efficient time integration in dislocation dynamics." Modelling and Simulation in Materials Science and Engineering22.2 (2014): 025003.

4. Bulatov, Vasily, and Wei Cai. Computer simulations of dislocations. Vol. 3. Oxford University Press on Demand, 2006.

5. Estrin, Y., H. S. Kim, and F. R. N. Nabarro. "A comment on the role of Frank–Read sources in plasticity of nanomaterials." Acta Materialia 55.19 (2007): 6401-6407.

6. Kunjomana, A. G., and E. Mathai. "Direct observation of Frank-Read sources in stoichiometric bismuth telluride crystals." Journal of materials science26.22 (1991): 6171-6175.

7. Sills, Ryan B., Amin Aghaei, and Wei Cai. "Advanced time integration algorithms for dislocation dynamics simulations of work hardening." Modelling and Simulation in Materials Science and Engineering 24.4 (2016): 045019.

8. Sedláček, R., et al. "Continuum theory of evolving dislocation fields." Philosophical Magazine 87.8-9 (2007): 1225-1260.

9. Van der Giessen, Erik, and Alan Needleman. "Discrete dislocation plasticity: a simple planar model." Modelling and Simulation in Materials Science and Engineering 3.5 (1995): 689.

10. Gomez-Garcia, D., B. Devincre, and L. P. Kubin. "Dislocation patterns and the similitude principle: 2.5 D mesoscale simulations." Physical review letters 96.12 (2006): 125503.

11. Yin, Jie, et al. "Computing dislocation stress fields in anisotropic elastic media using fast multipole expansions." Modelling and Simulation in Materials Science and Engineering 20.4 (2012): 045015.

12. Bulatov, Vasily V., Moon Rhee, and Wei Cai. "Periodic boundary conditions for dislocation dynamics simulations in three dimensions." MRS Proceedings. Vol. 653. Cambridge University Press, 2000.

13. Beardon, Alan F. The geometry of discrete groups. Vol. 91. Springer Science & Business Media, 2012.